Research article

JGS
Journal of the Geological Society

https://doi.org/10.1144/jgs2022-112 | Vol. 180 | 2023 | jgs2022-112

Age, duration and spatial distribution of ocean shields and rejuvenated volcanism: Fuerteventura and Lanzarote, Eastern Canaries

F. J. Perez-Torrado[1], J. C. Carracedo[1], H. Guillou[2*], A. Rodriguez-Gonzalez[1] and J. L. Fernandez-Turiel[3]

[1] Instituto de Estudios Ambientales y Recursos Naturales (i–UNAT), Universidad de Las Palmas de Gran Canaria (ULPGC), Las Palmas de Gran Canaria, Spain
[2] Laboratoire des Sciences du Climat et de l'Environnement/IPSL, CEA-CNRS-UVSQ, Bât. 714, Pièce 19, CEA-Orme des Merisiers-RD 128, F-91198 Gif-sur-Yvette Cédex, France
[3] Geosciences Barcelona, GEO3BCN, CSIC, Barcelona, Spain
FJP-T, 0000-0002-4644-0875; HG, 0000-0002-4811-7668
* Correspondence: herve.guillou@lsce.ipsl.fr

Abstract: Fuerteventura and Lanzarote form the oldest emerged part of the Eastern Canary Islands archipelago. Geologically, they can be considered a single edifice, constituting a continuous volcanic ridge extending 250 km from SW to NE. This study completes the dating and the determination of the magnetic stratigraphy of the shields and the rejuvenated volcanism of Fuerteventura and Lanzarote, refining the volcanic stratigraphy and cartography. The new unspiked K–Ar ages and magnetostratigraphy of Fuerteventura and Lanzarote indicate that these islands developed patterns similar to those of the Central and Western Canary Islands, building adjacent and successively superimposed basaltic shield volcanoes during the Miocene, between 20.19 ± 0.30 and 6.30 ± 0.11 Ma. The overlay of post-Miocene rejuvenated volcanism hinders determination of the extent and interrelationship of the shields. These materials constitute only a small fraction by volume but cover a large part of the islands. Despite this, it is confirmed that the disposition of the shields is opposite to the insular progression induced by the hotspot, suggesting the presence of some SW–NE propagation volcanic front or fracture to explain its direction of development.

Supplementary material: A description of the K–Ar method is available at https://doi.org/10.6084/m9.figshare.c.6641464

Received 25 July 2022; **revised** 3 April 2023; **accepted** 11 May 2023

Together with the Azores, Cape Verde and Madeira archipelagos, the Canary Islands form the Macaronesian group of oceanic volcanoes thought to result from independent mantle plumes on the moving eastern African plate (Carracedo *et al.* 2002; Carracedo and Troll 2016, 2021). Indeed, the Canary Islands show an age progression concordant with the displacement of the plate, with the Eastern islands (Fuerteventura and Lanzarote) forming the oldest edge of the emerged part of the Canarian Volcanic Province (Fig. 1) and the still older former islands composing a chain of seamounts extending towards the Iberian Peninsula (Geldmacher *et al.* 2005).

Most of the volume of oceanic hotspot islands, such as the Canaries, erupts in a first period of a few million years (Guillou *et al.* 1997, 2000; Carracedo *et al.* 2002; Garcia *et al.* 2010; Carracedo and Troll 2016, 2021; Williamson *et al.* 2019). This is the stage of shield building activity, during which eruption rates are high. Most of the volcanic edifices is formed, first the submarine pedestal and then the subaerial part. In this stage, the islands undergo a constructive phase in which growth through volcanic activity largely outpaces destruction through mass wasting (e.g. landslides) and erosion.

Even though mass wasting is an important process during the shield stage, islands continue to increase in size, despite short-term setbacks. The constructive phase proceeds in the subsequent cycle of volcanism commonly called the rejuvenated or post-erosional stage, during which volcanic eruptive rates are drastically lower (Clague and Dalrymple 1987; Carracedo *et al.* 1999, 2002; Carracedo and Troll 2016, 2021). The shield and rejuvenated building stages of volcanism are generally separated by extended periods of volcanic inactivity (or significantly reduced volcanism). Rejuvenated stage magmas can form extensive lava fields mantling the previous relief, hindering the observation of the underlying shield volcanoes, which are frequently reduced to small 'kipuka-type' outcrops. The term Hawaiian 'kipuka' refers to islands of forest cut off and surrounded by lava flows (Zimmerman 1948). The 'kipukas' are a feature characteristic of the central lower-relief areas of the old eastern Canary Islands of Fuerteventura and Lanzarote (Martínez Puebla *et al.* 2005). Finally, mass wasting and erosion outpace volcanic growth, and the volcanoes (islands) decrease in size until they are eroded to sea level and disappear, forming seamounts.

During 1971 and 1972, the combined efforts of the Lamont Doherty Geological Observatory at Columbia University (USA) and the Graduate School of Oceanography, University of Rhode Island (USA) carried out the first radiometric and palaeomagnetic study of the Canary Islands. K–Ar ages and geomagnetic polarities were determined from the Canaries' lavas to produce a quantitative within- and between-island stratigraphic framework (Abdel-Monem *et al.* 1971, 1972; Watkins 1973). This project was critical in improving the geochronological understanding of the Canarian Archipelago.

Starting in 1994, a joint French–Spanish programme with a similar approach was carried out by the group at the Centre des Faibles Radioactivités, CEA-CNRS, Gif-sur-Yvette, France (at present Laboratoire des Sciences du Climat et de l'Environnement/IPSL, CEA-CNRS-UVSQ, France), the Estación

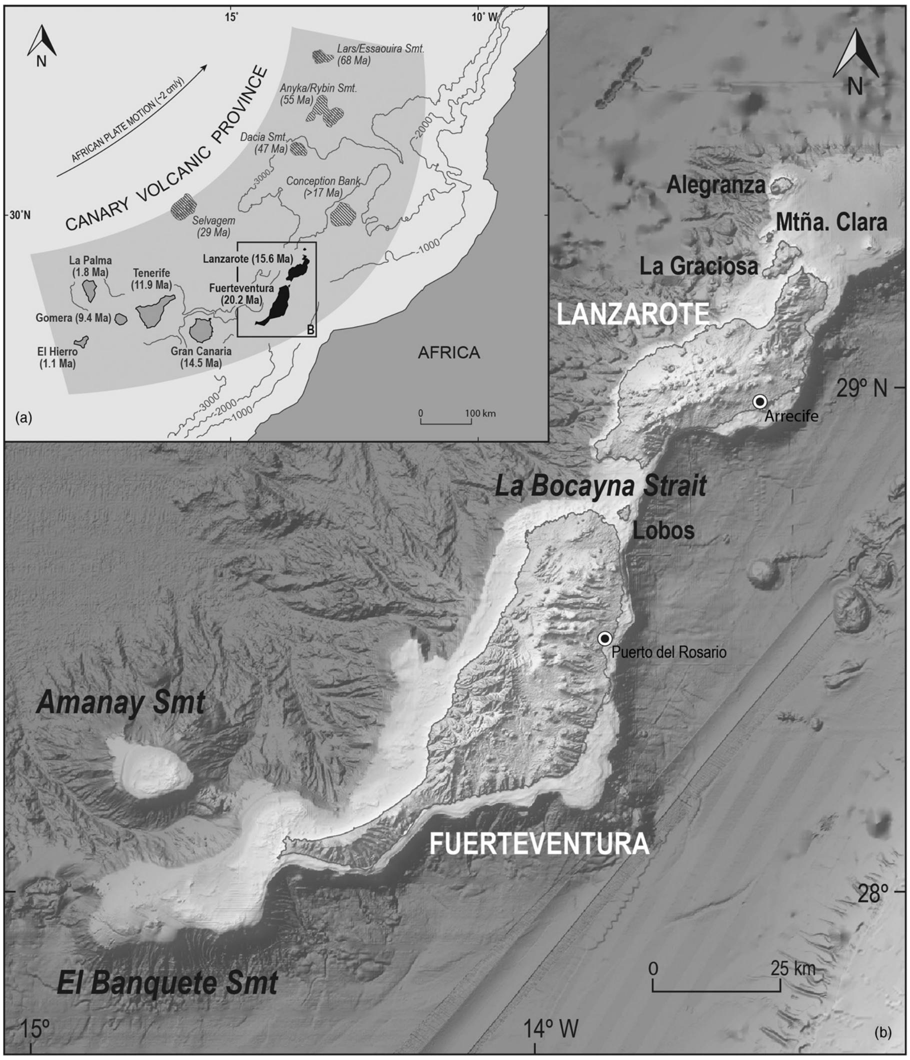

Fig. 1. (**a**) Location of Fuerteventura and Lanzarote on the eastern edge of the Canarian archipelago, the emerged part of a much longer chain of seamounts forming the northbound prolongation of the Canarian Volcanic Province (modified from Geldmacher *et al.* 2005). Numbers indicate the age of each island in Ma. (**b**) Bathymetry shows the islands of Fuerteventura and Lanzarote as a continuous SW–NE volcanic succession separated only by the shallow (−25 m) strait of La Bocayna. Two seamounts, Amanay and El Banquete, extend the Fuerteventura island southwards. Source: EMODnet Bathymetry Consortium (2020).

Volcanológica de Canarias, CSIC, Tenerife, Spain and the University of Las Palmas de Gran Canaria, Las Palmas, Spain. The use of geomagnetic polarities as a criterion in selecting rock samples for K–Ar determination proved to improve the geological significance of the radiometric ages considerably, as results could be compared with the established Geomagnetic Polarity Time Scale (GPTS) (Ogg 2020). Thus, combined palaeomagnetic and geochronological methods were very useful in defining magnetostratigraphic units and sections and, ultimately, composing and refining volcanic stratigraphy and mapping. Based on this framework, the French–Spanish team successively studied the islands of El Hierro, La Palma, La Gomera, Tenerife and Gran Canaria (Guillou *et al.* 1996, 1998, 2001, 2004*a*, *b*, 2011; Paris *et al.* 2005; Carracedo *et al.* 2007; Kissel *et al.* 2011, 2014, 2015).

Since the early K–Ar whole-rock ages of the Canary Islands published by Abdel-Monem *et al.* (1971, 1972), a wealth of new radiometric ages have been published, placing Canarian volcanism among the best chronologically constrained oceanic archipelagos (e.g. McDougall and Schmincke 1976; Staudigel *et al.* 1986; Ancochea *et al.* 1990, 1994, 2006; Thirlwall *et al.* 2000; Paris *et al.* 2005; Longpré *et al.* 2011; Carracedo and Troll 2021). Most of these samples focused on dating the old (Miocene–Pliocene) basaltic shield volcanoes, particularly the oldest outcropping subaerial formations, intending to test the alleged west to east age progression in the inception of the islands.

New radiometric ages of the Fuerteventura and Lanzarote subaerial growth were published (Meco and Stearns 1981; Féraud *et al.* 1985; Coello *et al.* 1992; Balcells Herrera *et al.* 1994; Ancochea *et al.* 1996; Meco *et al.* 2007; Mansour *et al.* 2023), but without any palaeomagnetic data and, consequently, these islands were the only ones left without correlation of radiometric ages and geomagnetic polarity history since the early determinations carried out by Abdel Monem and coworkers in 1971. The exception was the ages presented by Meco *et al.* (2007). The present study is intended to fill this gap and complete the radiometric dating and determination of the magnetic stratigraphy and mapping of Fuerteventura and Lanzarote shields and rejuvenated volcanism using the same sampling and laboratory procedures already tested by the above-mentioned French–Spanish team in the Western and Central Canaries, and thus complete the study of the entire Canary archipelago with similar and correlatable procedures. This will afford us between-island correlations, probably reducing important issues when comparing the ages of different groups with contrasting sampling criteria and dating methods. This feature is particularly critical in the older shield formations owing to the occurrence of older materials (including oceanic crust) or metasomatic alteration, processes that modify the K–Ar clock and lead to erroneous K–Ar ages.

Geological setting

The islands of Fuerteventura and Lanzarote differ from the other islands of the Canarian archipelago because they form the oldest, easternmost part of the emerged island chain composing the Canary Volcanic Province (Fig. 1a). In addition, they also contrast to the Central and Western Canaries because they do not form discrete volcanic edifices separated by abyssal depths of several thousand metres. Fuerteventura and Lanzarote are separated by a narrow strait (La Bocayna or La Bocaina strait) with depths in some parts not exceeding 25 m (Fig. 1b). Lanzarote is the northeastern prolongation of Fuerteventura, and shows similarities in geological and geochronological observations, particularly the age and distribution of their Miocene shield volcanoes described in this paper (Balcells Herrera *et al.* 2006*a*, *b*).

Similar shallow depths form the southwesternmost edge of the volcanic ridge, where two shallow-depth seamounts, the Amanay and El Banquete seamounts, prolong the edifice of Fuerteventura southwards. A comparable shallow-depth marine erosion platform extends Lanzarote 50 km to the NE, including the islets of La Graciosa, Alegranza, Montaña Clara, Roque del Este and Roque del Oeste (locally known as the Chinijo archipelago), giving the Eastern Canary Volcanic Ridge a total length of 250 km (Fig. 1).

Classic stratigraphic division on Fuerteventura comprises two major structural and petrological stages: the Basal Complex and the Subaerial Volcanic Series (I–IV) of Neogene to Quaternary ages (e.g. Fúster *et al.* 1968*a*; Stillman *et al.* 1975). The Basal Complex includes a Mesozoic oceanic crust with a thick sedimentary sequence, submarine volcanism and coeval intrusions, mainly intense NNE–SSW-trending sheeted dyke swarms (e.g. Stillman *et al.* 1975; Ancochea *et al.* 1996; Fernandez *et al.* 1997). The Miocene Series I is formed by the growth of three large volcanic complexes: Northern, Central and Southern (Coello *et al.* 1992; Ancochea *et al.* 1993, 1996; Balcells Herrera *et al.* 1994). Later, Balogh *et al.* (1999) divided the geological evolution of the island into four main stages: (A) Mesozoic oceanic crust with sedimentary rocks; (B) Eocene–Oligocene Submarine and Transitional Volcanic Group and Intrusions; (C) Miocene Subaerial Volcanic Complexes and Intrusions; (D) Pliocene–Quaternary sedimentary and volcanic complex. Stages A, B and part of C form the Basal Complex; stage C is equivalent to Series I of Fúster *et al.* (1968*a*); stage D includes Series II–IV of Fúster *et al.* (1968*a*).

There are no outcrops of the Basal Complex on the island of Lanzarote. Fúster *et al.* (1968*b*) initially divided the subaerial sequences into Series I–IV, similarly to the Fuerteventura division. Coello *et al.* (1992) maintained this division, relating the Miocene Series I to the growth of two volcanic complexes: Ajaches in the south and Famara in the north.

In the framework of the main stages of growth of volcanic ocean islands, as defined in Hawaii (Clague and Sherrod 2014), Carracedo and Troll (2016, 2021) divided the subaerial volcanic evolution of Fuerteventura and Lanzarote into the shield (including Series I), postshield and rejuvenated stages (including Series II–IV).

Methods

The combination of the Geomagnetic Polarity Time Scale (GPTS) (Ogg 2020) and radiometric dating to define the main stratigraphic units has proven to be valuable in other Canary Islands (e.g. Guillou *et al.* 1996, 1998, 2001, 2004*a*, *b*; Paris *et al.* 2005; Kissel *et al.* 2011, 2014, 2015). Mapping and correlating geomagnetic polarity units allow volcanic events determined by radiometric methods to be grouped, significantly reducing the number of age determinations.

Palaeomagnetism

The preliminary definition of the geomagnetic polarity units on the islands of Fuerteventura and Lanzarote was carried out in the field using portable fluxgate magnetometers. Oriented samples were taken with standard procedures (portable drill, solar orientation and magnetic compass) for nearly all samples selected for radiometric dating. Two standard pilot cores from each site were prepared for palaeomagnetic measurement. Thermal and alternating field (AF) stepwise demagnetization were performed on these pilot samples. The direction and intensity of the magnetization were analysed using spinner magnetometers. We used the GPTS from TimeScale Creator, version 8.0 (https://timescalecreator.org/index/index.php; released January 2021). The age model for version 8.0 is from Gradstein *et al.* (2020).

K–Ar dating

The measurements of K and Ar were carried out on the microcrystalline groundmass, which is considered representative of the moment of solidification of the lavas. Only rocks without traces of alteration, with an aphanitic texture and very little or no vesicularity were selected. A description of the K–Ar method is given in the Supplementary material. All dated samples have a loss on ignition (LOI) of less than 1.5%. Analytical procedures have been described by Guillou *et al.* (1996).

Results

Magnetic mapping and stratigraphy were defined based on the geological map of Fuerteventura and Lanzarote published by Fúster *et al.* (1968*a*, *b*) and updated by the Spanish Geological Survey (IGME) in the framework of the MAGNA project (Balcells Herrera *et al.* 2006*a*, *b*). Palaeomagnetic results reported only for those units that have been dated are given in Figures 2–13 and Tables 1–4.

Magnetozones recorded during the shield stage

Geomagnetic polarity surveys carried out on the shield volcanoes of Fuerteventura and Lanzarote (Abdel-Monem *et al.* 1971; Fúster and Carracedo 1979) showed relatively limited, well-defined and correlatable magnetozones, similar to those previously observed in the Central and Western Canaries (Abdel-Monem *et al.* 1972; Carracedo 1979; Perez-Torrado *et al.* 1995; Guillou *et al.* 1996, 1998, 2004*a*, *b*; Carracedo *et al.* 2001, 2007; Paris *et al.* 2005). Lavas from the shield volcanoes of the Eastern islands present a comparatively low number of magnetozones (Figs 2–5), and their correlation with the corresponding older part of the GPTS strongly depends on the accuracy and precision of their radiometric ages.

Shield stage volcanism of Fuerteventura

Three overlapping shield volcanoes built the island of Fuerteventura: the Northern (La Oliva) Shield, the Central (Tuineje) Shield and the Southern (Jandía) Shield (Fig. 2).

The Northern (La Oliva) Shield extended the island towards the north, resting unconformably at its southern edge over the Central (Tuineje) Shield and the submarine Basal Complex (Fig. 2). The bottom sequence is formed by an extensive, normal polarity magnetozone sampled at the foot and top of Los Corraletes mountain (FV-26 and FV-27). Towards the south, the eruptive activity of the shield is more complex, probably related to more discontinuous alternating periods of eruptive activity and repose, probably characterizing its late shield-stage volcanism. This period shows several magnetozones alternatively of opposite polarities. The sequence is capped by two overlapping magnetozones of normal (FV-12) and reversed (FV-10) polarities (cross-section 1–1’ in Fig. 4).

The Central (Tuineje) Shield is the oldest feature in the Canaries where tectonic processes, including endogenous uplift, exposed a shield volcano’s submarine growth and emergence (Fernandez *et al.* 1997). This shield comprises three stages of volcanic growth (submarine, transitional and subaerial), resting on a block of Mesozoic oceanic crust (Fernandez *et al.* 1997; Gutiérrez *et al.* 2006). The uplifted Mesozoic oceanic crust, the submarine, transitional and subaerial volcanism, and the associated plutonic

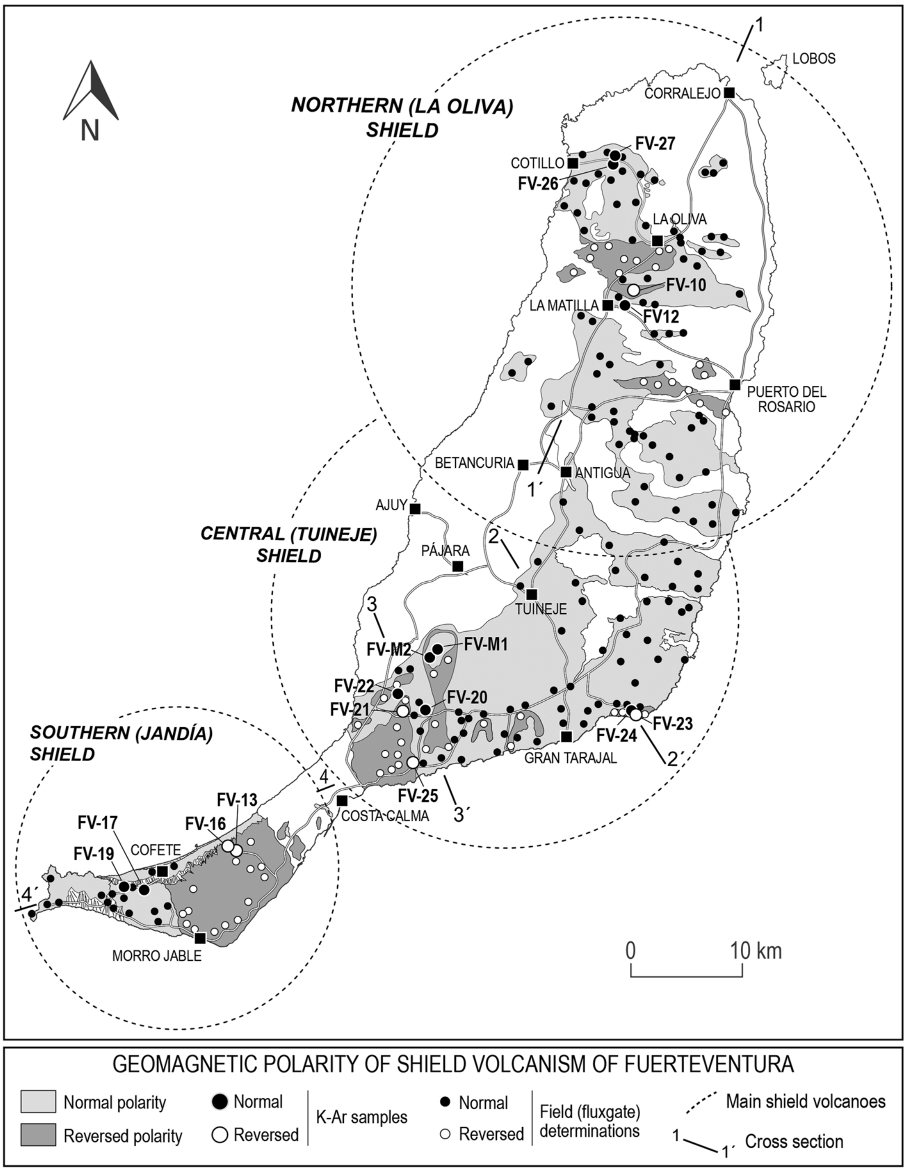

Fig. 2. Magnetozones mapped in the shield stage volcanism of Fuerteventura. Magnetic polarity defined on-site using portable fluxgate magnetometers. Samples selected for K–Ar dating are shown with their geomagnetic polarities.

bodies and dykes compose the so-called Basal Complex of Fuerteventura (Fúster *et al.* 1968*a*; Stillman *et al.* 1975; Fernandez *et al.* 1997; Balogh *et al.* 1999; Gutiérrez *et al.* 2006). In this paper, only the subaerial Miocene volcanism has been considered (Fig. 2).

The Central Shield, which crops out south of Antigua, appears to be composed of two polarity units: a basal magnetozone of normal polarity forming the more significant part of the volcanic edifice, topped by a reversed polarity unit cropping out mainly in the southernmost part of the volcano (Fig. 2). However, in some cases, volcanic sequences apparently of the same polarity were considered as potentially different magnetozones when presenting contrasting features (density and dyke directions, unconformities), probably related to different periods of volcanism, and accordingly were separately sampled for radiometric dating. Field relations of these magnetozones are outlined in the cross-sections 2–2’ and 3–3’ of Figure 4, where at least three distinct magnetozones are defined.

The majority of the section cutting through the middle of the Central (Tuineje) Shield, from Tuineje to the Faro de la Entallada cliff (cross-section 2–2’ in Fig. 4), corresponds to an extensive normal polarity unit (sample FV-24) topped by a reversed polarity magnetozone (sample FV-23). Field observations suggest that the normal polarity unit with sample FV-24 correlates with the basal normal polarity magnetozone shown in cross-section 3–3’ in Figure 4. Thus, the overlying magnetozones of reversed (FV-25 and FV-21) and normal (FV-22, FV-20, FV-M1 and FV-M2) polarities seem to belong to a different, younger stage of volcanism.

The Southern (Jandía) Shield forms the Jandía peninsula in the southwestern part of Fuerteventura (Fig. 2). Intensive, long-lasting erosion, apparently increased by northbound massive lateral collapses (Stillman 1999; Krastel *et al.* 2001; Casillas and Martin 2021), has exposed the volcano’s interior as an 810 m high lava sequence unconformably overlying the Central (Tuineje) Shield at its eastern boundary (see cross-section 4–4’ in Fig. 4). Two magnetozones have been distinguished, a lower normal polarity unit (FV-17) and an upper reversed polarity unit (FV-13 and FV-16). However, the lava sequence forming the tip of the peninsula, although presenting normal polarity (FV-19) conceivably equivalent to that of the basal unit (FV-17), seems to belong to a different magnetozone, as an unconformity separates the two stratigraphic sections (different orientation of dykes and dip of lava sequences in the two units).

Shield stage volcanism of Lanzarote

Similar to Fuerteventura, the island of Lanzarote is composed of three main volcanic edifices: the Northern (Famara) Shield, the Central Shield and the Southern (Los Ajaches) Shield (Fig. 3).

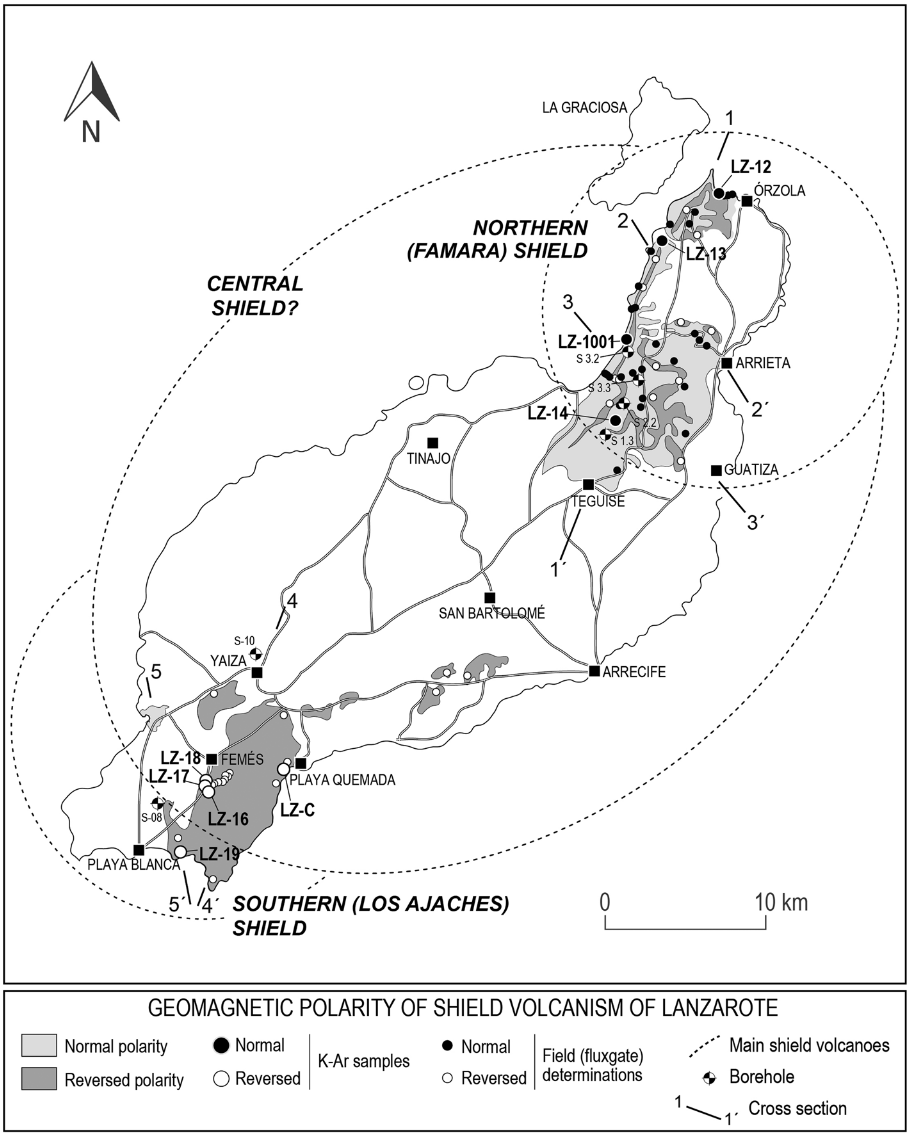

Fig. 3. Magnetozones mapped in the shield stage volcanism of Lanzarote. Samples selected for K–Ar dating are shown with their geomagnetic polarities. Boreholes data from SPA-15 (1975).

The Northern (Famara) Shield characteristic features are the frequent short episodes of low inclinations and geomagnetic excursions (Fig. 5). However, the majority of the volcanic sequence is composed of a normal polarity (sample LZ-14) magnetozone, separated by a sequence of reversed polarity from the lower magnetozone of normal polarity (samples LZ-12 and LZ-13) (Fig. 3 and cross-sections 1–1’, 2–2’ and 3–3’ in Fig. 5).

A cluster of rock-coring boreholes drilled to estimate groundwater reserves in Famara provided valuable information on the magnetic stratigraphy of the volcano (inset in Fig. 5). Core logs from two of these rotary drill cores (S-3.2 and S-3.3) run several metres above the present sea level (cross-sections 1–1’ and 3–3’ in Fig. 5) into a layer providing a low proportion of core recovered, probably related to sediments derived from long periods of erosion (Guillou *et al.* 1996). Reversed polarity magnetozones and episodes of low geomagnetic inclination (LI) alternate with normal polarity sequences, probably indicating the volcano’s growth through pulses of volcanism interspersed with periods of repose and erosion.

What remains of the Southern Shield of Lanzarote forms the deeply eroded, 560 m high volcanic Los Ajaches massif. Only a reversed polarity magnetozone seems to include the entire shield, implying a rapid growth of the volcano. As shown in cross-sections 4–4’ and 5–5’ in Figure 5, samples for radiometric dating were taken in stratigraphic order (LZ-19, LZ-18, LZ-17, LZ-16). A challenge arises when trying to fit the normal polarity lava outcrop at Salinas del Janubio within the magnetic stratigraphy of the Southern (Los Ajaches) Shield. According to Meco *et al.* (2007), this normal polarity lava flow (*LZ-22*) is separated from underlying lavas by a Miocene marine abrasion platform, covered with fossil-bearing calcarenites and marine conglomerates with abundant rounded and rubefacted basaltic clasts (cross-section 5–5’ in Fig. 5). Although its location would suggest that this unit should belong to the Southern (Los Ajaches) Shield, the mismatched geomagnetic polarity and the unconformity makes this explanation unlikely. Borehole S-10, located about 2 km north of Yaiza (Sánchez-Guzmán and Abad 1986), cuts normal polarity lavas (cross-section 4–4’ in Fig. 5), separated at about 15 m asl (above sea level) from the underlying Southern (Los Ajaches) Shield reversed polarity lavas by a sediment-filled marine bed similar to the Salinas del Janubio outcrop (Carracedo and Rodriguez Badiola 1993). The old age of the shield, and the subsequent prolonged eruptive repose and erosion, point to the dismantling of a substantial volume of the Los Ajaches volcanic edifice and the subsequent development of an extensive marine abrasion platform and sediments, characteristic facies of the windward coasts in the old volcanic series. These deposits (Balcells Herrera *et al.* 2006*b*) are practically identical to those observed in Fuerteventura (Balcells Herrera *et al.* 2006*a*) and have already been described (Hausen 1959, 1967; Lecointre *et al.* 1967; Klug 1968). A feasible explanation is to associate this mismatching outcrop woth lava flows encircling the eroded Los

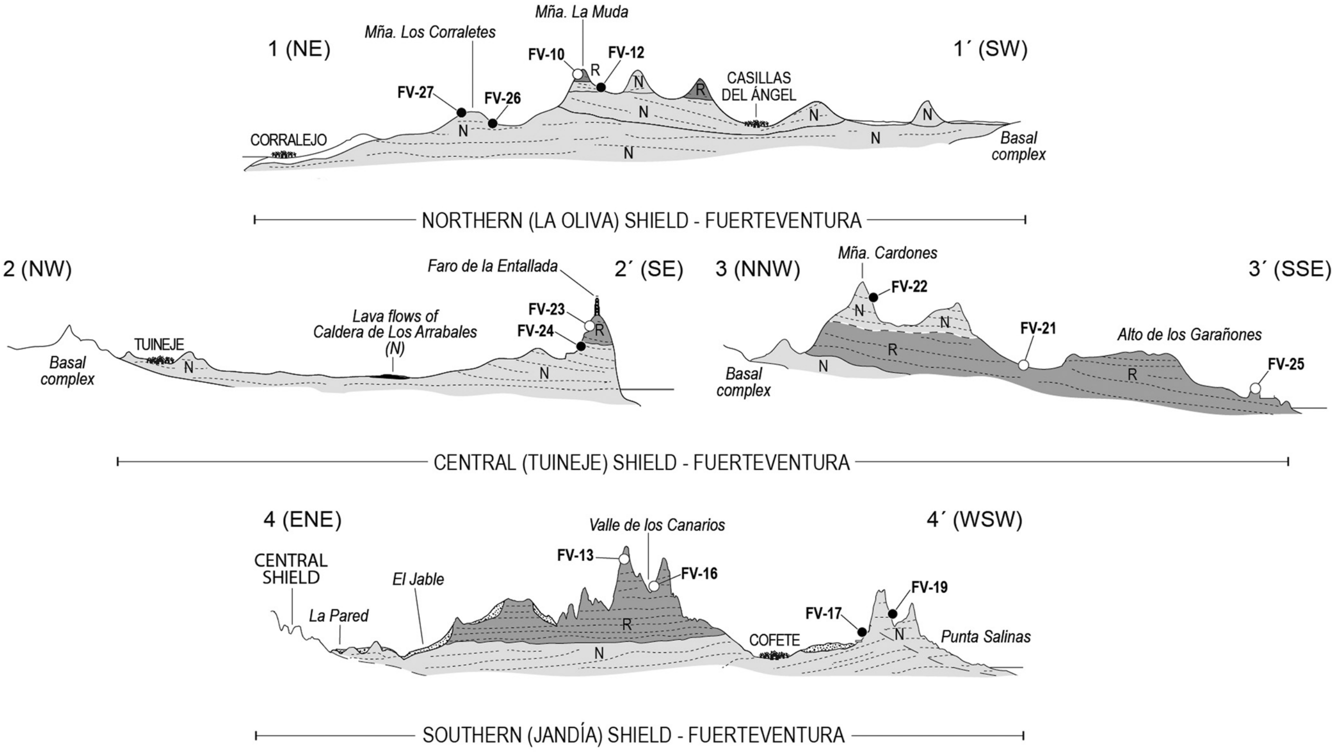

Fig. 4. Idealized cross-sections, nonlinears and vertical scale exaggerated, showing the correlation of magnetozones from shield-stage volcanic rocks of Fuerteventura. Filled circles indicate normal polarity (N); open circles indicate reversed polarity (R).

Ajaches massif to rest over the Miocene abrasion platform, probably corresponding to a Central Shield interspersed between the older Southern (Los Ajaches) Shield and the younger Northern (Famara) Shield (Fig. 3).

Magnetozones of the rejuvenated volcanism

Rejuvenated volcanism shows a contrasting pattern in the distribution of volcanism in time and space and the number of

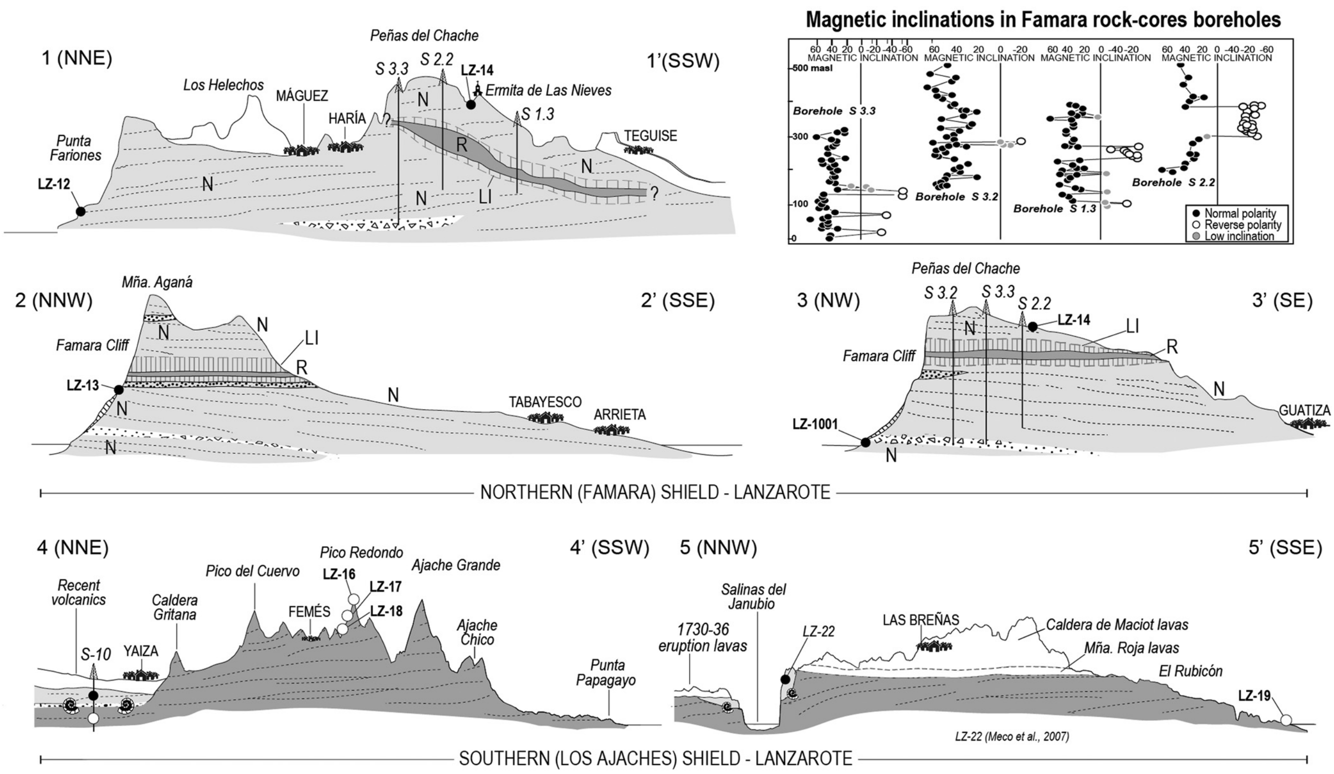

Fig. 5. Idealized cross-sections, nonlinears and vertical scale exaggerated, showing the correlation of magnetozones from shield-stage volcanic rocks of Lanzarote. Filled circles indicate normal polarity (N); open circles indicate reversed polarity (R); LI indicates low geomagnetic inclination. Inset: changes in geomagnetic inclinations observed in cores recovered from boreholes drilled to study groundwater resources in Famara (SPA-15 1975; Carracedo and Soler 1995). Reversed polarity magnetozones and episodes of low geomagnetic inclination (LI) alternate with normal polarity sequences.

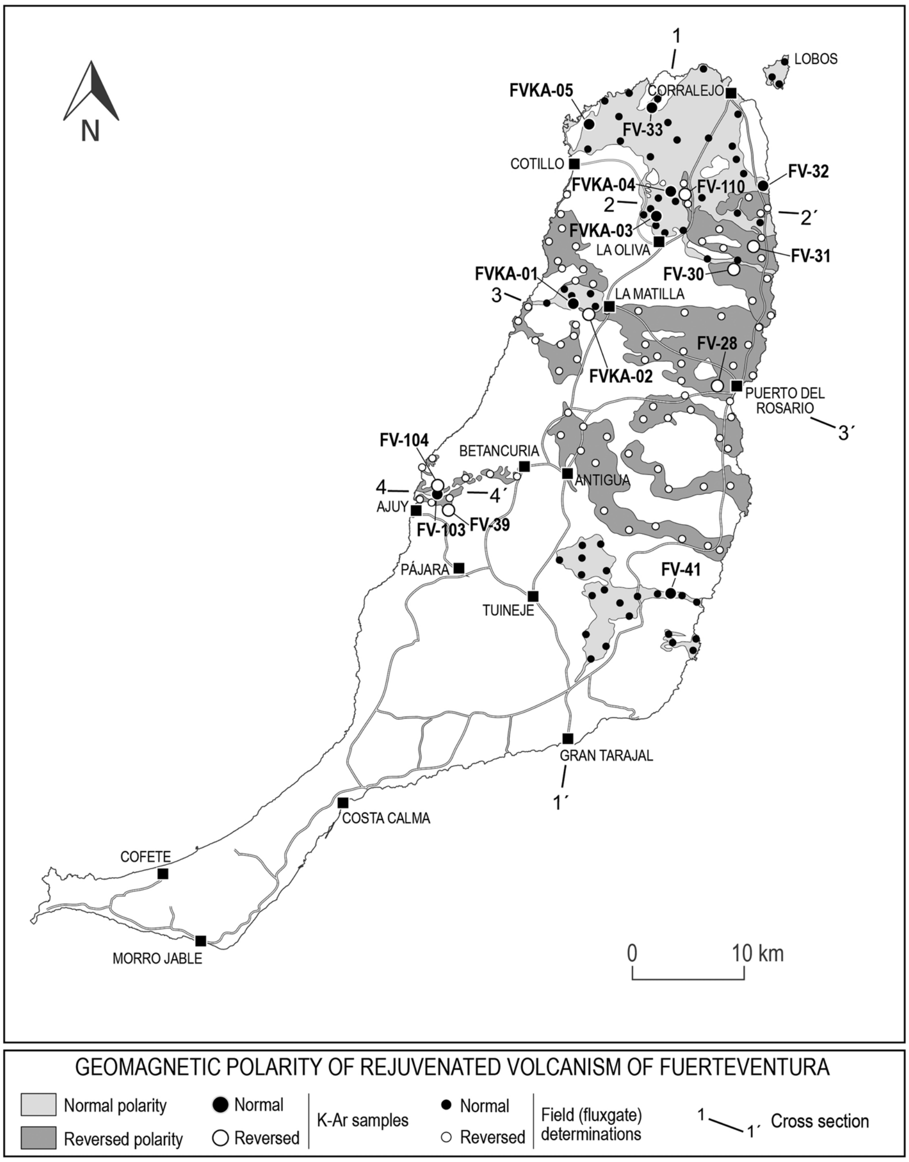

Fig. 6. Magnetozones mapped in Fuerteventura's rejuvenated (post-Miocene) volcanism. Magnetic polarity defined on-site using portable fluxgate magnetometers. Samples selected for K–Ar dating are shown with their geomagnetic polarities.

magnetozones. Although this volcanism is significant in extension, it is interesting to verify whether, as in most oceanic volcanic islands, the duration, volume and eruptive rates are only a small fraction of the shield-stage volcanism (Figs 6 and 7).

Rejuvenated volcanism of Fuerteventura

Rejuvenated volcanism crops out only in Fuerteventura's central and northern parts as fissural basaltic eruptions. The more complex set of magnetozones is associated with the volcanic rocks that crop out from Betancuria to Ajuy, where the erosive remains of the lava flows are embedded in an ancient ravine (Figs 6 and 8). Close to Ajuy, a basal reversed polarity sequence (samples FV-38 and FV-39) is overlain by normal (FV-103) and reversed (FV-104) polarity lavas, and the whole sequence rests on the Basal Complex (cross-section 4–4' in Fig. 8).

Rejuvenated volcanism drifted northward, forming a cluster of fissure vents and extensive lava fields, consistently of reversed polarity (samples FVKA-02, FV-28, FV-30, FV-31 and FV-110). Identical polarity does not necessarily mean that these eruptions correspond to a single magnetozone. On the contrary, these eruptions show contrasting conservation states, suggesting that they may be of different ages. Normal polarity lavas (FVKA-01, FVKA-03, FVKA-04, FVKA-05, FV-32, FV-33 and FV-41) consistently coincide with the best-preserved eruptions, seemingly corresponding to the Brunhes chron (<780 ka). They constitute only a small fraction of the rejuvenated volcanism (cross-sections 1–1', 2–2' and 3–3' in Fig. 8).

Rejuvenated volcanism of Lanzarote

The distribution of rejuvenated volcanism in Lanzarote extends over the entire island, with eruptive centres arranged in NE–SW-oriented fissures, and the islets of the Chinijo archipelago (de la Nuez *et al.* 1997), located above the NE marine erosion platform of the island (Fig. 7). The large surface area covered by recent eruptions, particularly the 1730–1736 event, gives the misleading appearance of a young island, being locally known as 'the island of the thousand volcanoes'. The great majority of Lanzarote was constructed during the Miocene, the rejuvenated volcanism representing only a small fraction of the total volume of the island (Fúster *et al.* 1968*b*; Coello *et al.* 1992; Balcells Herrera *et al.* 2006*b*; Carracedo and Troll 2016).

Unlike Fuerteventura, the bulk of the rejuvenated volcanism of the island of Lanzarote and NE islets was emplaced mostly during the Brunhes normal polarity chron (samples LZ-101, LZ-103, LZ-104, LZ-105, LZ-106, LZ-23, LZ-24, LZ-A and LZ-B), with only two eruptions of reversed polarity, the Montaña Roja and Volcán de Teguise (samples LZ-15 and LZ-20), probably erupted during the Matuyama chron (Figs 7 and 9).

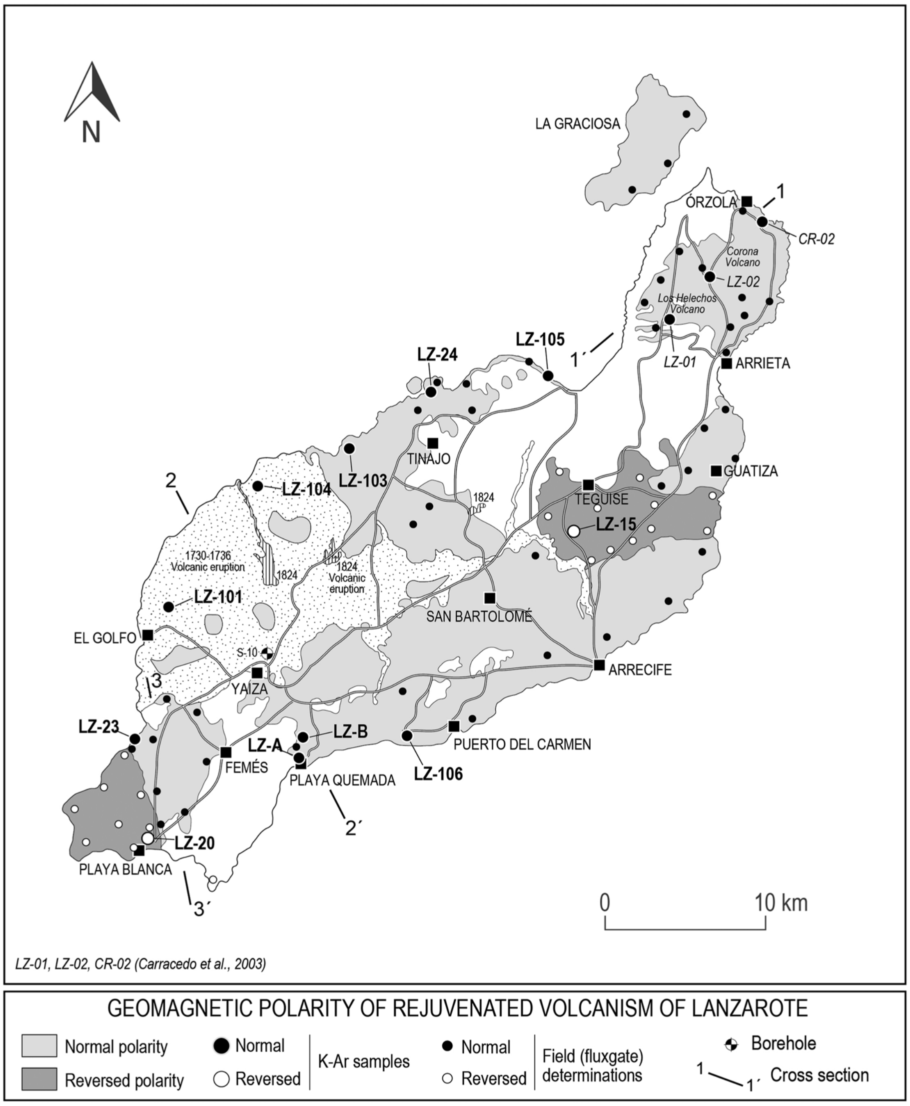

Fig. 7. Magnetozones mapped in Lanzarote's rejuvenated (post-Miocene) volcanism. Magnetic polarity defined on-site using portable fluxgate magnetometers. Samples selected for K–Ar dating are shown with their geomagnetic polarities.

K–Ar ages of shield volcanism

The K–Ar age determinations for the shield volcanism of Fuerteventura and Lanzarote are reported in Tables 1 and 2 and Figures 10–14. This volcanism took place over a long period starting during the early Miocene and covering several magnetozones.

K–Ar ages of shield-stage volcanism: Fuerteventura

The oldest age obtained for the Central (Tuineje) Shield, at the foot of Montaña Cardones (Table 1, Fig. 10), confirms that this shield constitutes the initial stage of creating the island. This sampling point yielded a reversed polarity and an age of 20.19 ± 0.30 Ma (sample FV-21) that should be considered as one of the oldest basal magnetozones of the Central (Tuineje) Shield (cross-sections 2–2' and 3–3' in Fig. 4).

Considering the oldest (20.19 ± 0.30 Ma) and youngest (13.73 ± 0.21 Ma) ages obtained for the Central (Tuineje) Shield, a period of growth of *c.* 6.5 myr is revealed. This feature is supported by field observations; namely, the numerous discontinuities separating the magnetozones, which represent temporal gaps (cross-sections 2–2' and 3–3' in Fig. 4), as also indicated by previous researchers (Coello *et al.* 1992; Ancochea *et al.* 1993, 1996). Similarly, the old age and extended growth period of this shield are of the same order of magnitude as those obtained for the underlying submarine shield (i.e. 31–23 Ma; Gutiérrez *et al.* 2006). Two million years after the initiation of the central shield, about 18.09 ± 0.21 myr ago, the construction of the northern shield (La Oliva) began, and it continued until 13.09 ± 0.20 Ma. This shield extended the island towards the north, resting unconformably at its southern edge over the Central (Tuineje) Shield and the submarine Basal Complex (Fig. 2 and cross-section 1–1' in Fig. 4).

Radiometric dating of the field-defined magnetozones constrained the development of the Southern (Jandía) Shield between 15.44 ± 0.23 and 13.72 ± 0.21 Ma (Table 1, Fig. 10). However, some inconsistencies may occur between the K–Ar ages and the magnetic polarities of some samples. Sample FV-17 has a normal polarity whereas it is dated at 15.34 ± 0.23 Ma, an age that coincides with a period of reverse geomagnetic polarity (Fig. 10). Nevertheless, taking into account the error on the K–Ar date, the age and the magnetic polarity can be reconciled. Noteworthy is the age of the sample FV-19 (13.72 ± 0.21 Ma, normal polarity), forming the westernmost and youngest part of the Southern (Jandía) Shield, coherent with the existence of a discordance in this area as observed in the field (cross-section 4–4' in Fig. 4).

In summary, based on our ages, the volcanic activity started with the edifice construction of the central (Tuineje) shield 20.19 ± 0.30 Ma ago and contined until 13.73 ± 0.21 Ma. From 18.09 ± 0.27 Ma, the construction of the northern (La Oliva) shield began and continued for 5 myr, during which both the central and northern shields were active. This activity increased from 15.44 ± 0.23 Ma, the date of the first eruptions of the southern shield. Thus, the three

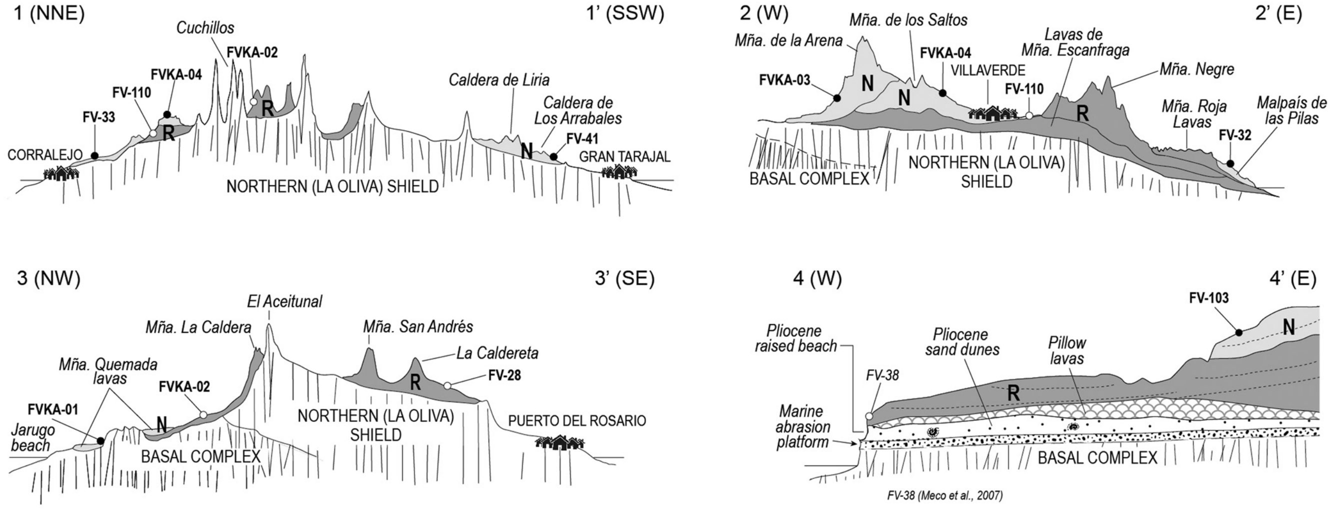

Fig. 8. Idealized cross-sections, nonlinears and vertical scale exaggerated, showing magnetozones in Fuerteventura's rejuvenated (post-Miocene) volcanism. Samples selected for K–Ar dating are shown with their geomagnetic polarities. Filled circles indicate normal polarity; open circles indicate reversed polarity.

shields were active between 15.44 ± 0.23 and 13.72 ± 0.21 Ma (cross-section A–A' in Fig. 13).

K–Ar ages of shield-stage volcanism: Lanzarote

The construction of Lanzarote was initiated 15.61 ± 0.23 myr ago with the construction of the Southern (Los Ajaches) Shield (Table 2, Fig. 11). The section along the flank of Pico Redondo mountain yielded ages of 15.60 ± 0.23 Ma at 320 m asl, 15.45 ± 0.23 Ma at 360 m and 14.06 ± 0.21 Ma at the top (480 m) of the sequence (Table 2 and cross-sections 4–4' in Fig. 5 and B–B' in Fig. 13).

Ages of the Lanzarote Northern Shield (Famara) vary from 7.23 ± 0.11 to 6.30 ± 0.11 Ma (Table 2), a short period (<1 myr) probably indicating a general decrease in eruptive rates at this later stage of the formation of Lanzarote.

No previous mention has been made of the existence of a central shield in Lanzarote, as previous researchers included the Miocene volcanic rocks in Series I of Fúster *et al.* (1968*b*) (e.g. Abdel-Monem *et al.* 1971; Coello *et al.* 1992). Only a few small, isolated outcrops of Series I were reported and mapped in the central part of Lanzarote, a vast flat region almost entirely mantled by rejuvenated volcanism between the old massifs of Los Ajaches and Famara. However, as already mentioned, borehole S-10, located at the central part of the island, crossed Miocene volcanic rocks that may correspond to a deeply mass-wasted central shield (cross-section 4–4' in Fig. 5 and cross-section 2–2' in Fig. 9). This 240 m deep borehole crossed Miocene lavas 23 m b.s.l. (below sea level), topped at +15 m by a sediment-filled marine bed similar to the Salinas del Janubio outcrop (Carracedo and Rodriguez Badiola 1993). Prolonged eruptive repose and erosion, probably enhanced by lateral collapses, easily account for dismantling a substantial volume of the volcanic edifice and developing an extensive marine abrasion platform and sediments, characteristic facies of the windward coasts in the Series I (Meco *et al.* 2007).

Therefore, there is little evidence other than our K–Ar ages to suggest the existence of a central shield volcano forming the extensive lowland at the centre of Lanzarote, interbedded between the older Southern and younger Northern shields (Fig. 3 and cross-section B–B' in Fig. 13). Additional evidence favouring the existence of this central shield is provided by the dating of a basaltic flow at the lower section of the Famara cliff, dated at 10.89 ± 0.23 Ma (Table 2, sample LZ-1001; see cross-section 3–3' in Fig. 5). This basal lava unit of Famara is separated from the overlying volcanic series by a Miocene fossil-bearing calcarenite bed (close to sea level at the northern foot of the Famara cliff near

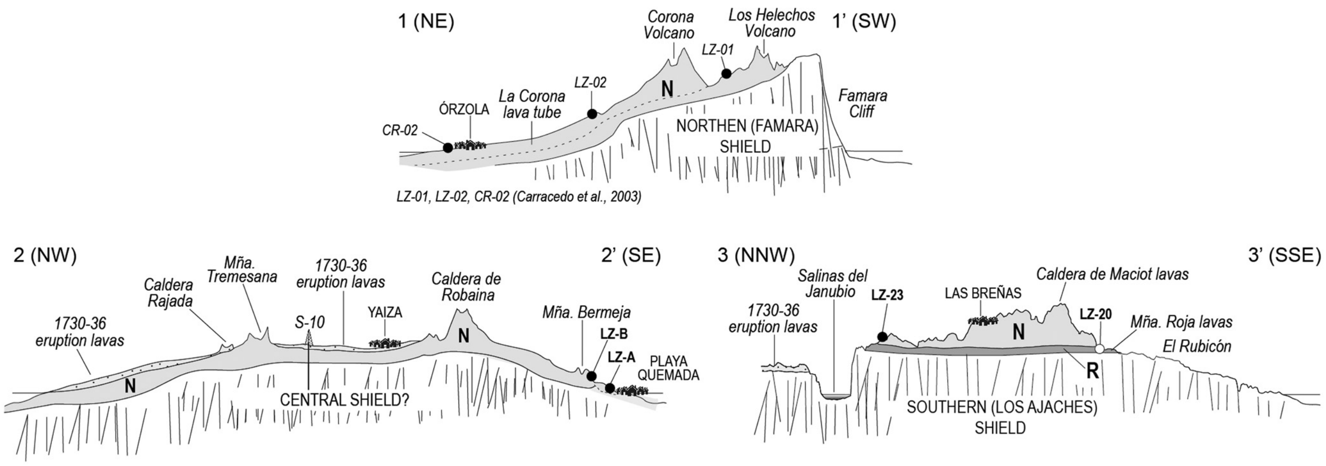

Fig. 9. Idealized cross-sections, nonlinears and vertical scale exaggerated, showing magnetozones in Lanzarote's rejuvenated (post-Miocene) volcanism. Samples selected for K–Ar dating are shown with their geomagnetic polarities. Borehole S-10 data from Sánchez-Guzmán and Abad (1986). Filled circles indicate normal polarity; open circles indicate reversed polarity.

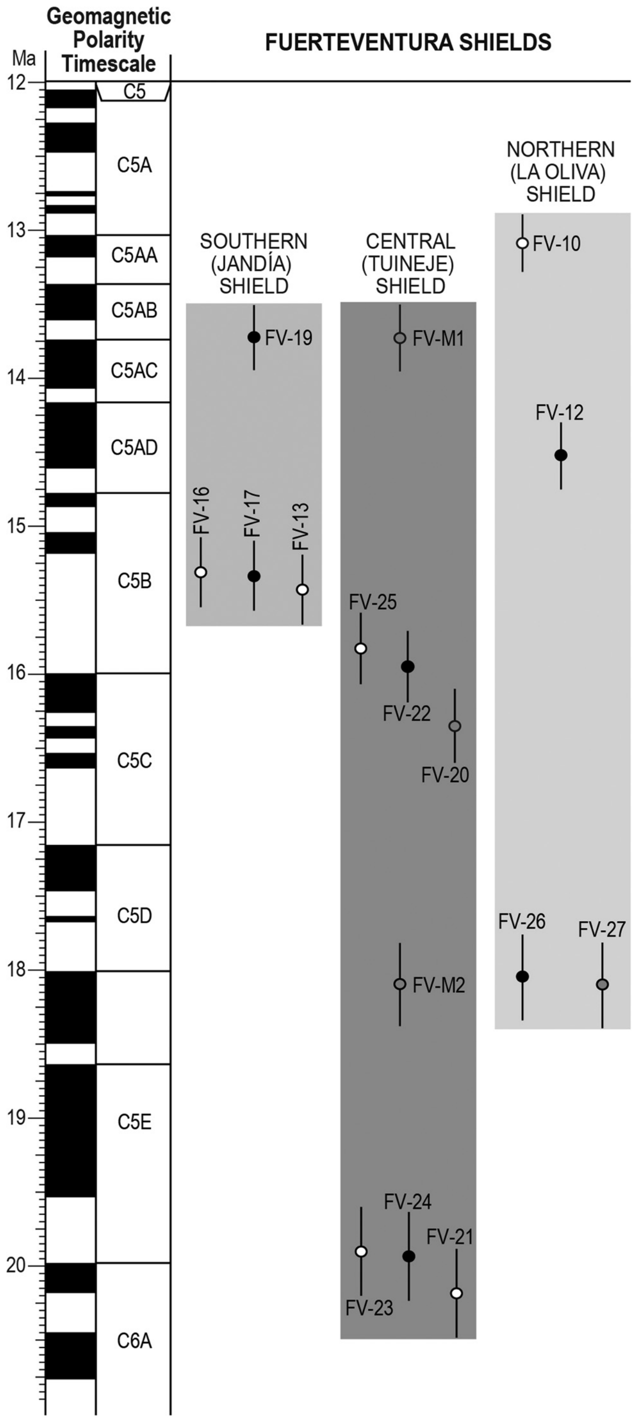

Fig. 10. Time distribution of K–Ar ages and uncertainties (bars) obtained from Fuerteventura shield volcanism, and comparison with the Geomagnetic Polarity Time Scale (GPTS). Filled circles indicate normal polarity, open circles indicate reversed polarity; grey circles indicate low geomagnetic inclination.

Casa del Inglés and the northernmost tip of Famara, at Punta Fariones), suggesting that this 10.89 myr old lava flow may be the NE prolongation of the Central Shield.

The already mentioned difficult fit of the normal polarity lava outcrop at Salinas del Janubio (sample *LZ-22* of Meco *et al.* 2007) within the magnetic stratigraphy of the Southern (Los Ajaches) Shield is validated by the age of this sample (8.89 ± 0.13 Ma), clearly at odds with the much older Los Ajaches massif. This age supports this lava flow as an erosion remnant from an alleged central shield (see Table 2 and cross-sections 5–5' in Fig. 5 and B–B' in Fig. 13).

In summary, all the ages obtained for the shield-stage volcanism of Lanzarote are coherent with their relative stratigraphic positions and with their geomagnetic polarity. Unlike Fuerteventura, the growth of each independent shield on Lanzarote has a shorter duration (≤2 myr) with probably temporal gaps between them.

K–Ar ages of rejuvenated volcanism

The correlation between Fuerteventura and Lanzarote field-determined magnetozones and K–Ar ages (Tables 3 and 4, Fig. 12) is significantly more straightforward in the rejuvenated

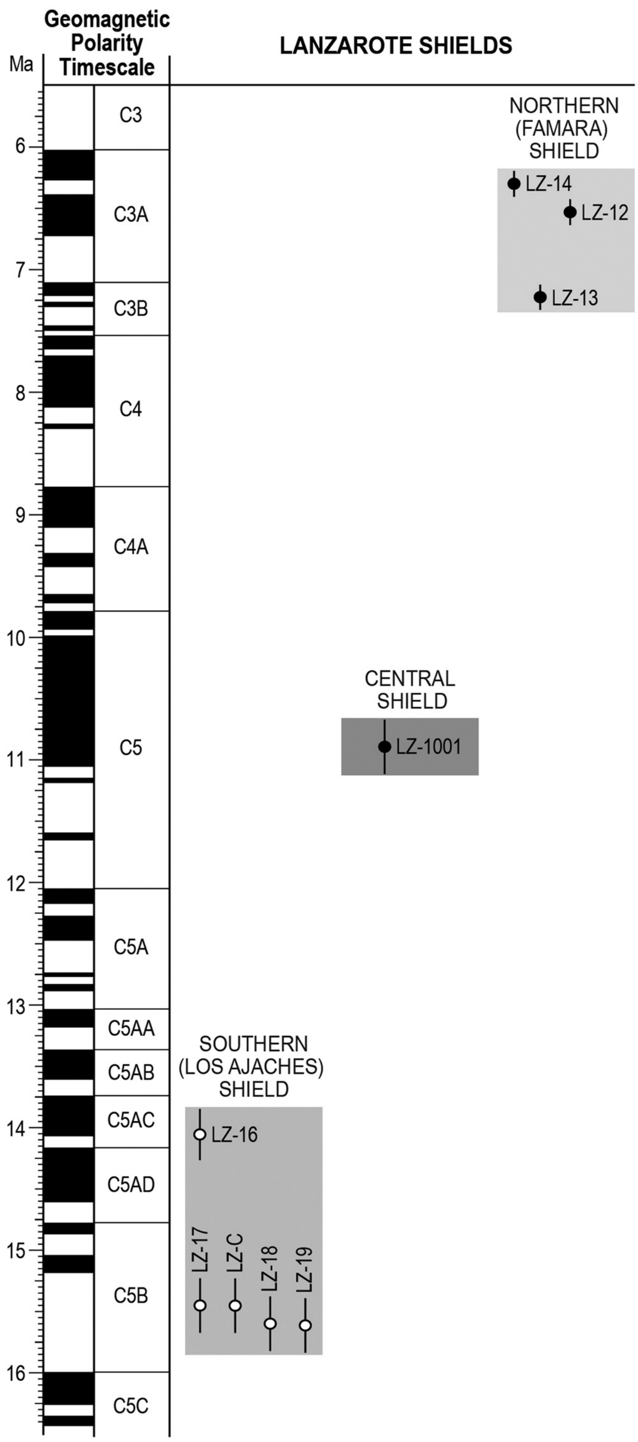

Fig. 11. Time distribution of K–Ar ages and uncertainties (bars) obtained from Lanzarote shield volcanism, and comparison with the Geomagnetic Polarity Time Scale (GPTS). Filled circles indicate normal geomagnetic polarity; open circles indicate reversed geomagnetic polarity.

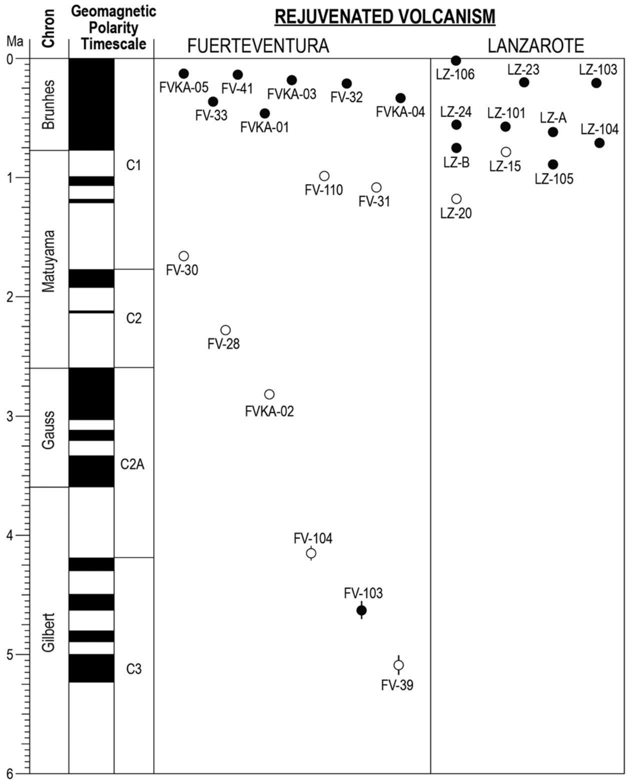

Fig. 12. Time distribution of K–Ar ages and uncertainties (bars) obtained from Fuerteventura and Lanzarote rejuvenated volcanism, and comparison with the Geomagnetic Polarity Time Scale (GPTS). Filled circles indicate normal geomagnetic polarity; open circles indicate reversed geomagnetic polarity. Uncertainty bars less than 0.05 are included in the circles.

stage. Younger ages imply better preservation of volcanic features and shorter duration with fewer geomagnetic polarities, facilitating stratigraphic and magnetostratigraphic correlations (Figs 12 and 14). This is particularly evident in Lanzarote, where eruptions occurred only in the Matuyama and Brunhes chrons (Figs 12 and 14).

K–Ar ages of rejuvenated volcanism: Fuerteventura

Rejuvenated volcanism in Fuerteventura started about 5 myr ago during the Pliocene. The most recent expression of volcanism dates from the Holocene, and unlike Lanzarote, no eruptions have occurred during modern history (see Table 3). Pliocene volcanism is preserved as basaltic lava remnants that flowed in the lower course of the Barranco de Malpaso, which ends in Playa de Ajuy (cross-section 4–4’ in Fig. 8). The duration of this volcanic activity (*c.* 1 myr) encompassed the two oldest geomagnetic excursions within the Gilbert chron (Fig. 11). Then, during the Gauss chron, close to la Matilla, the four cinder cones erupted, one of which is dated at 2.82 ± 0.04 Ma (sample FVKA-02). Later, during the Matuyama and Brunhes chrons, the activity continued sporadically (cross-section 1–1’ in Figs 8, 12 and 14).

The age of sample FV-41 (0.136 ± 0.008 Ma) appears older than the degree of preservation of the lava field, as stratigraphic–geomorphological relationships indicate. This sample comes from the lava field Malpaís Grande, forming a volcanic group with the so-called Malpaís Chico, about 200 m north, and Malpaís de Los Toneles, about 3 km to the SE. All the lava fields in this volcanic group show the same degree of preservation, with scoriaceous surfaces without caliche or soil cover. The Malpaís de Los Toneles generated a significant lava delta, with its submarine prolongation well marked by the bathymetric curves. Following the same geomorphological criteria as used in the western and central islands (Carracedo *et al.* 2001, 2007; Carracedo and Troll 2016; Rodriguez-Gonzalez *et al.* 2018, 2022), the eruption that produced the Malpaís de Los Toneles had to take place during the present interglacial, and thus has an age of less than 20 ka. This data point agrees with the stratigraphic section raised by Petit-Maire *et al.* (1986) at the bottom of the Pozo Negro Valley, about 500 m from the coast. In this section, the lava flow of the FV-41 sample covers aeolian sands dated at 23 600 ± 500 years BP.

Despite this evidence contrary to the K–Ar age obtained for this sample, it should be noted that the Malpaís Grande lava flow did not develop a lava delta, as it has not been recorded on land or in bathymetric curves, or it was eroded and therefore would be older than the lava delta of the Malpaís de Los Toneles.

K–Ar ages of rejuvenated volcanism: Lanzarote

Except for the Pleistocene (Matuyama chron) Montaña Roja, at the southern tip of Lanzarote, Volcán de Teguise and a lava flow at Caleta de Famara covered by dunes, all rejuvenated volcanism of Lanzarote dates from the Pleistocene–Holocene Brunhes epoch (see Table 4 and Fig. 7). These eruptions, dated between 1.17 ± 0.02 Ma and 18 ± 7 ka and mainly focused on the central part of the islands,

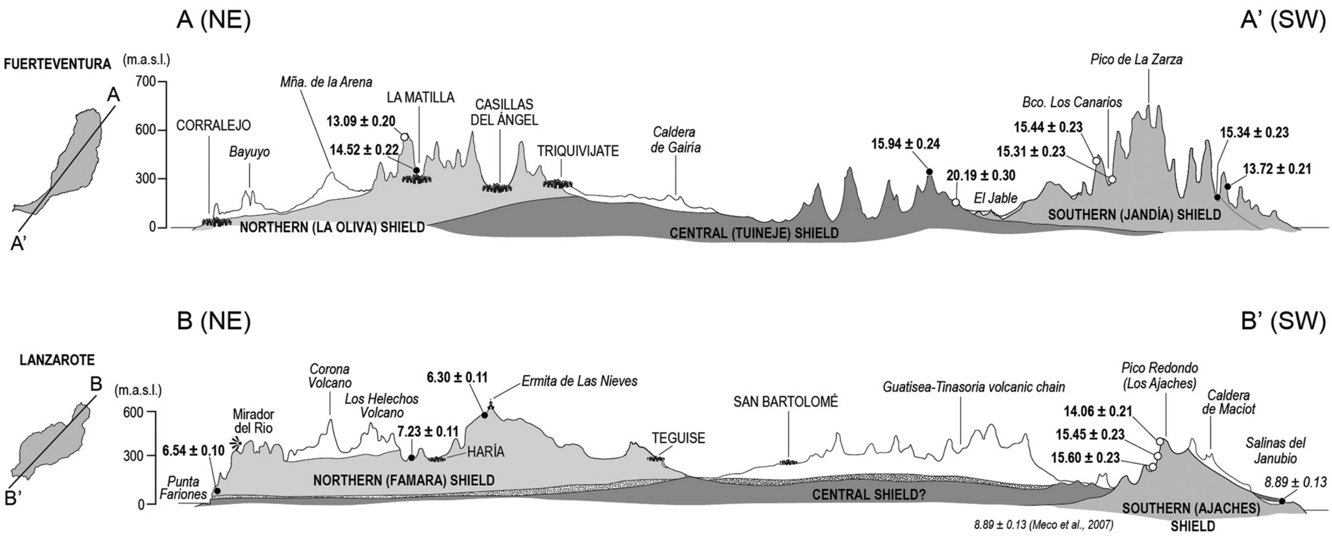

Fig. 13. Idealized NE to SW cross-sections, nonlinears and vertical scale exaggerated, of Fuerteventura (A–A’) and Lanzarote (B–B’) indicating the K–Ar ages obtained for their shield stage volcanism. Filled circles indicate normal polarity; open circles indicate reversed polarity; ages in Ma.

Table 1. *Site locations, magnetic declinations, inclinations and polarities, and K–Ar ages of samples belonging to shield stage volcanism of Fuerteventura*

Sample	Locality (m a.s.l.), lat./long. (WGS84)	Declination (deg.)	Inclination (deg.)	Polarity	K^* (wt%)	Weight molten (g)	$^{40}Ar^*$ (%)	$^{40}Ar^*$ (10^{-12} mol g^{-1})	Weighted mean ± 1σ	Age (Ma) ± 2σ
Northern (La Oliva) Shield										
FV-10	Mña. La Muda (600 m)	191.7	−48.9	R	1.079 ± 0.011	0.87325	50.220	24.244 ± 0.123		
	28.5700/−13.9581					0.79290	56.337	24.941 ± 0.126	24.585 ± 0.088	13.09 ± 0.20
FV-12	Mña. La Muda (290 m)	0.4	36.9	N	1.702 ± 0.017	1.06048	64.037	43.273 ± 0.217		
	28.5629/−13.9673					0.43090	43.796	42.743 ± 0.226	43.018 ± 0.156	14.52 ± 0.22
FV-26	Mña. Los Corraletes (150 m)	251.7	58.9	N	1.453 ± 0.014	0.98201	26.048	44.842 ± 0.234		
	28.6670/−13.9764					0.56627	18.004	46.731 ± 0.260	45.689 ± 0.174	18.04 ± 0.27
FV-27	Mña. Los Corraletes (230 m)	79.5	9.3	N (LI)	0.855 ± 0.009	0.78663	35.540	26.807 ± 0.138		
	28.6686/−13.9738					1.08285	30.380	27.117 ± 0.137	26.964 ± 0.097	18.09 ± 0.27
Central (Tuineje) Shield										
FV M1	Morro de la Leña (370 m)	354.2	6.1	N (LI)	1.254 ± 0.013	0.47299	24.520	30.119 ± 0.163		
	28.2789/−14.1233					0.45297	27.430	29.816 ± 0.160	29.965 ± 0.114	13.73 ± 0.21
FV-25	Los Garañones (70 m)	172.4	−40.9	R	1.096 ± 0.011	0.69565	63.325	29.881 ± 0.151		
	28.1816/−14.1679					0.72369	53.381	30.539 ± 0.154	30.203 ± 0.108	15.82 ± 0.24
FV-22	Mña. Cardones (500 m)	81.5	48.4	N	0.722 ± 0.007	0.98159	44.937	19.974 ± 0.101		
	28.2427/−14.1647					0.98160	42.505	20.126 ± 0.102	20.049 ± 0.072	15.94 ± 0.24
FV-20	Cuchillo Negro (190 m)	151.6	6	N (LI)	1.353 ± 0.013	0.78372	51.236	38.890 ± 0.196		
	28.2357/−14.1401					0.71548	52.725	38.188 ± 0.194	38.536 ± 0.138	16.35 ± 0.25
FV M2	Morro de la Leña (245 m)	298.1	11.9	N (LI)	1.237 ± 0.012	0.92488	61.165	38.876 ± 0.196		
	28.2758/−14.1257					1.03522	78.000	39.138 ± 0.196	39.007 ± 0.139	18.09 ± 0.27
FV-23	Faro La Entallada (180 m)	141.8	−61.7	R	1.021 ± 0.010	0.86741	45.231	34.802 ± 0.175		
	28.2308/−13.9487					0.74275	66.027	36.113 ± 0.182	35.433 ± 0.126	19.90 ± 0.30
FV-24	Faro La Entallada (100 m)	341	27.9	N	2.906 ± 0.029	0.71771	87.961	101.63 ± 0.503		
	28.2323/−13.9522					0.80022	76.752	100.42 ± 0.508	101.02 ± 0.357	19.94 ± 0.30
FV-21	Mña Cardones (260 m)	327.8	−55.6	R	0.739 ± 0.007	1.02575	31.470	26.311 ± 0.133		
	28.2374/−14.1596					0.63609	50.616	25.750 ± 0.130	26.024 ± 0.093	20.19 ± 0.30
Southern (Jandía) Shield										
FV-19	Cofete track (220 m)	335.6	21.9	N	1.237 ± 0.012	0.84535	45.652	29.827 ± 0.151		
	28.0928/−14.4318					0.72081	45.911	29.276 ± 0.148	29.546 ± 0.106	13.72 ± 0.21
FV-16	Valle de los Canarios (310 m)	210.2	−37.3	R	0.838 ± 0.008	0.77947	61.530	22.558 ± 0.114		
	28.1240/−14.3297					0.82808	48.254	22.137 ± 0.112	22.345 ± 0.080	15.31 ± 0.23
FV-17	Cofete track (170 m)	329.9	48.9	N	1.262 ± 0.013	0.98377	43.363	33.379 ± 0.167		
	28.0911/−14.4206					0.54878	49.495	34.094 ± 0.173	33.725 ± 0.112	15.34 ± 0.23
FV-13	Valle de los Canarios (390 m)	182	−25.4	R	0.714 ± 0.007	1.16342	56.335	19.346 ± 0.097		
	28.1156/−14.3257					1.06139	55.208	19.062 ± 0.096	19.202 ± 0.068	15.44 ± 0.23

Ages are calculated from the weighted mean of two independent $^{40}Ar^*$ measurements.
Polarity: N, normal; R, reversed; LI, low geomagnetic inclination.

Table 2. *Site locations, magnetic declinations, inclinations and polarities, and K–Ar ages of samples belonging to shield stage volcanism of Lanzarote*

Sample	Locality (m a.s.l.), lat./long. (WGS84)	Declination (deg.)	Inclination (deg.)	Polarity	K^* (wt%)	Weight molten (g)	$^{40}Ar^*$ (%)	$^{40}Ar^*$ (10^{-12} mol g^{-1})	Weighted mean ± 1σ	Age (Ma) ± 2σ
Northern (Famara) Shield										
LZ-14	Ermita de Las Nieves (590 m)	13.2	40.3	N	0.490 ± 0.005	1.13735	26.349	0.537 ± 0.003		
	29.1066/−13.5293					1.04189	28.539	0.535 ± 0.003	0.536 ± 0.002	6.30 ± 0.11
LZ-12	Punta Fariones (30 m)	2.1	52.3	N	0.789 ± 0.008	0.95768	23.620	0.914 ± 0.005		
	29.2255/−13.4643					0.79538	31.485	0.880 ± 0.005	0.896 ± 0.004	6.54 ± 0.10
LZ-13	Famara north cliff (310 m)	354.4	49.8	N	0.440 ± 0.004	0.9317	21.680	0.545 ± 0.003		
	29.1956/−13.4951					1.09021	24.429	0.560 ± 0.003	0.553 ± 0.002	7.23 ± 0.11
Central Shield[1]										
LZ-1001	Famara north cliff (10 m)	345.2	48.1	N	0.955 ± 0.010	1.03754	47.727	1.833 ± 0.009		
	29.1403/−13.5255					1.00204	42.638	1.785 ± 0.009	1.808 ± 0.007	10.89 ± 0.23
Southern (Los Ajaches) Shield										
LZ-16	Pico Redondo (480 m)	167.2	−12.1	R	0.731 ± 0.007	0.92810	40.859	1.794 ± 0.009		
	28.9022/−13.7737					1.05467	54.504	1.785 ± 0.009	1.789 ± 0.006	14.06 ± 0.21
LZ-17	Pico Redondo (360 m)	160.4	−39.6	R	0.955 ± 0.010	1.13618	46.424	2.578 ± 0.013		
	28.9047/−13.7824					1.15258	56.377	2.563 ± 0.013	2.570 ± 0.009	15.45 ± 0.23
LZ-C	Playa Quemada (65 m)	169.3	−35.9	R	0.921 ± 0.009	0.98287	50.225	2.491 ± 0.013		
	28.9102/−13.7372					1.00642	51.835	2.466 ± 0.012	2.478 ± 0.009	15.45 ± 0.23
LZ-18	Pico Redondo (320 m)	181.4	−47.3	R	1.096 ± 0.011	1.13540	54.979	2.965 ± 0.015		
	28.9052/−13.7824					0.96378	67.479	2.993 ± 0.015	2.979 ± 0.011	15.60 ± 0.23
LZ-19	Playa Las Coloradas (0 m)	164.4	−27.3	R	0.755 ± 0.008	0.97677	62.266	2.049 ± 0.010		
	28.8585/−13.8024					1.06152	66.527	2.056 ± 0.010	2.052 ± 0.007	15.61 ± 0.23

Ages are calculated from the weighted mean of two independent $^{40}Ar^*$ measurements.
Polarity: N, normal; R, reversed.
[1]Assuming this age is related to the Central Shield of Lanzarote.

Table 3. *Site locations, magnetic declinations, inclinations and polarities, and K–Ar ages of samples belonging to rejuvenated volcanism of Fuerteventura*

Sample	Locality (m a.s.l.), lat./long. (WGS84)	Declination (deg.)	Inclination (deg.)	Polarity	K^* (wt%)	Weight molten (g)	$^{40}Ar^*$ (%)	$^{40}Ar^*$ (10^{-12} mol g^{-1})	Weighted mean ± 1σ	Age (Ma) ± 2σ
FVKA-05	Llanos de Tostón (20 m)[1]			N[2]	0.698 ± 0.007	1.60050	0.765	0.166 ± 0.015		
	28.7096/−14.0002					1.45738	0.695	0.159 ± 0.017	0.163 ± 0.011	0.134 ± 0.013
FV-41	Bco. de Pozo Negro (30 m)	3.2	44.3	N	0.930 ± 0.009	1.41306	1.778	0.205 ± 0.013		
	28.3288/−13.9113					1.55629	1.855	0.203 ± 0.011	0.220 ± 0.009	0.136 ± 0.008
FVKA-03	Mña. de La Arena (195 m)			N[2]	0.943 ± 0.009	1.37605	1.355	0.298 ± 0.015		
	28.6392/−13.9380					1.59964	1.485	0.307 ± 0.015	0.302 ± 0.011	0.185 ± 0.010
FV-32	Malpaís de las Pilas (10 m)	3.8	29.6	N	1.337 ± 0.013	1.22230	3.505	0.504 ± 0.016		
	28.6566/−13.8316					2.21284	4.787	0.495 ± 0.008	0.497 ± 0.007	0.214 ± 0.005
FVKA-04	Rincón de Cuba (150 m)			N[2]	0.630 ± 0.006	1.37653	2.819	0.374 ± 0.009		
	28.6550/−13.9191					1.47630	2.317	0.375 ± 0.012	0.375 ± 0.007	0.343 ± 0.010
FV-33	Tableros del Guirre (50 m)	358.4	55.9	N	0.573 ± 0.006	0.99488	0.907	0.333 ± 0.022		
	28.7225/−13.9376					1.27149	2.215	0.372 ± 0.017	0.357 ± 0.014	0.359 ± 0.020
FVKA-01	Mña. Quemada (140 m)[3]			N[2]	1.159 ± 0.012	1.49879	0.788	0.902 ± 0.008		
	28.5625/−13.9996					1.05591	0.833	0.949 ± 0.008	0.926 ± 0.006	0.460 ± 0.040
FV-110	Cueva del Llano (150 m)	195.6	−34.0	R	0.623 ± 0.006	1.21281	4.768	1.076 ± 0.017		
	28.6530/−13.9028					1.00134	3.919	1.067 ± 0.019	1.072 ± 0.012	0.992 ± 0.021
FV-31	Bco. del Cavadero (50 m)	210.7	−34.7	R	1.029 ± 0.010	1.16602	6.635	1.979 ± 0.021		
	28.6026/−13.8441					0.96743	5.203	1.862 ± 0.026	1.933 ± 0.016	1.08 ± 0.02
FV-30	La Calderetilla (150 m)	162.7	−32.2	R	0.905 ± 0.009	0.97066	15.934	2.629 ± 0.019		
	28.5869/−13.8752					1.19534	23.997	2.584 ± 0.016	2.603 ± 0.012	1.66 ± 0.03
FV-28	Bco. de Lucas (90 m)	176.1	−15.7	R	0.731 ± 0.007	1.23230	15.662	2.917 ± 0.020		
	28.4977/−13.8879					1.13377	14.598	2.852 ± 0.021	2.887 ± 0.014	2.28 ± 0.04
FVKA-02	Tablero Blanco (160 m)			R[2]	1.098 ± 0.011	1.44058	21.382	5.386 ± 0.030		
	28.5571/−13.9900					1.53253	18.340	5.373 ± 0.032	5.380 ± 0.022	2.82 ± 0.04
FV-104	Ajuí (80 m)	186.6	−29.4	R	0.830 ± 0.008	0.72953	16.107	6.047 ± 0.039		
	28.4021/−14.1398					0.61634	12.899	5.915 ± 0.040	5.982 ± 0.028	4.15 ± 0.06
FV-103	Ajuí (60 m)	303.6	55.5	N	0.888 ± 0.009	1.19725	21.480	7.178 ± 0.040		
	28.4015/−14.1398					0.98600	18.549	7.082 ± 0.042	7.133 ± 0.029	4.63 ± 0.07
FV-39	FV-621 road (70 m)	178.9	−25.5	R	0.739 ± 0.007	0.93467	30.566	6.519 ± 0.038		
	28.3933/−14.1296					0.98474	21.764	6.540 ± 0.037	6.529 ± 0.026	5.09 ± 0.08

Ages are calculated from the weighted mean of two independent $^{40}Ar^*$ measurements.
Polarity: N, normal; R, reversed.
[1]Above aeolian sand.
[2]Field polarity using portable fluxgate magnetometer.
[3]Above calcrete.

Table 4. *Site locations, magnetic declinations, inclinations and polarities, and K–Ar ages of samples belonging to the rejuvenated volcanism of Lanzarote*

Sample	Locality (m a.s.l.), lat./long. (WGS84)	Declination (deg.)	Inclination (deg.)	Polarity	K^* (wt%)	Weight molten (g)	$^{40}Ar^*$ (%)	$^{40}Ar^*$ (10^{-12} mol g^{-1})	Weighted mean ± 1σ	Age (Ma) ± 2σ
LZ-106	Puerto del Carmen (20 m)			N[1]	0.689 ± 0.007	1.00415	0.113	0.019 ± 0.011		
	28.9224/−13.6716					1.51700	0.220	0.023 ± 0.007	0.022 ± 0.006	0.018 ± 0.007
LZ-23	Las Breñas (40 m)	348.6	54.6	N	0.598 ± 0.006	1.02953	1.973	0.193 ± 0.014		
	28.9273/−13.8242					2.56150	2.431	0.213 ± 0.008	0.209 ± 0.006	0.201 ± 0.010
LZ-103	Las Cambuesas (110 m)			N[1]	0.689 ± 0.007	1.50411	3.713	0.239 ± 0.004		
	29.0814/−13.6981					3.00918	3.358	0.248 ± 0.004	0.244 ± 0.003	0.204 ± 0.005
LZ-24	La Costa del Río (10 m)	2.5	49.4	N	1.087 ± 0.011	1.14524	3.865	1.015 ± 0.035		
	29.1125/−13.6526					1.09109	10.027	1.059 ± 0.013	1.053 ± 0.012	0.558 ± 0.012
LZ-101	Mña. Quemada (80 m)			N[1]	0.898 ± 0.009	1.51452	4.447	0.894 ± 0.007		
	28.9918/−13.8161					1.50624	3.907	0.889 ± 0.010	0.892 ± 0.004	0.574 ± 0.010
LZ-A	Playa Quemada (5 m)	354.6	46.3	N	0.897 ± 0.009	1.02208	3.906	0.953 ± 0.020		
	28.9066/−13.7321					1.07300	4.888	0.996 ± 0.019	0.976 ± 0.014	0.627 ± 0.015
LZ-104	Llano de los Morales (40 m)			N[1]	1.021 ± 0.010	1.49241	8.585	1.300 ± 0.007		
	29.0616/−13.7554					1.50304	11.440	1.232 ± 0.009	1.268 ± 0.006	0.716 ± 0.011
LZ-B	Mña. Bermeja (50 m)	354.7	31	N	0.722 ± 0.007	0.93713	4.612	0.944 ± 0.018		
	28.9133/−13.7310					2.13799	5.924	0.946 ± 0.012	0.946 ± 0.010	0.755 ± 0.015
LZ-15	Nazaret (200 m)	175.8	−31.9	R	1.337 ± 0.013	1.08098	10.381	1.799 ± 0.019		
	29.0357/−13.5591					1.58438	14.096	1.808 ± 0.014	1.805 ± 0.011	0.778 ± 0.013
LZ-105	Caleta de Famara (10 m)			N[1]	0.905 ± 0.009	1.51337	10.174	1.398 ± 0.009		
	29.1196/−13.5718					1.50599	9.819	1.400 ± 0.010	1.399 ± 0.007	0.891 ± 0.014
LZ-20	Playa Blanca (10 m)	197.8	−39.6	R	1.121 ± 0.011	1.05762	14.880	2.377 ± 0.018		
	28.8620/−13.8323					1.01220	13.640	2.223 ± 0.017	22.77 ± 0.012	1.17 ± 0.02

Ages are calculated from the weighted mean of two independent $^{40}Ar^*$ measurements.
Polarity: N, normal; R, reversed.
[1]Field polarity using portable fluxgate magnetometer.

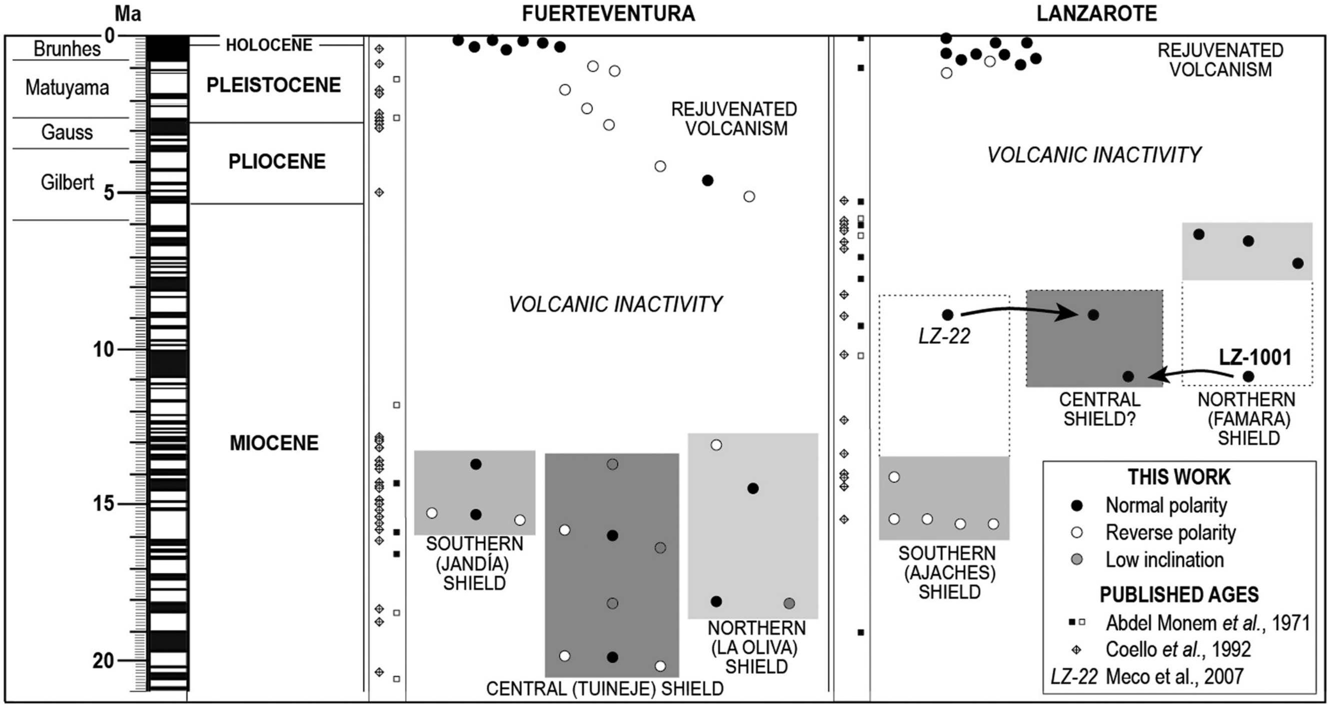

Fig. 14. Time distribution of K–Ar ages obtained from Fuerteventura and Lanzarote shield and rejuvenated volcanism, and comparison with the Geomagnetic Polarity Time Scale (GPTS). Filled circles indicate normal polarity; open circles indicate reversed polarity; grey circles indicate low geomagnetic inclination. Ages for these islands published by other researchers (Abdel-Monem *et al.* 1971; Coello *et al.* 1992) are indicated for comparison. The initial emerged part of the Fuerteventura shields developed in clearly distinct periods, although the end is practically coeval. In Lanzarote, the 8.89 Ma age (sample *LZ-22*) from a lava flow encircling the Southern (Los Ajaches) Shield is interpreted to correspond to the Central Shield; the same is the case for sample LZ-1001, 10.89 Ma age, from a basal lava in the Northern (Famara) Shield.

form SW–NE-trending lineaments of basaltic vents, including the extensive lavas of the 1730–1736 historical eruption (Fig. 7 and cross-section 2–2’ in Fig. 9). The immediately preceding volcanic activity took place in Famara (cross-section 1–1’ in Fig. 9), with the Los Helechos volcanic group and the overlying La Corona volcano respectively dated at 91 ± 2 and 21 ± 7 ka (Carracedo *et al.* 2003). An interesting feature of the latter eruption is a 7.5 km long and up to 35 m diameter lava tube, with a final 1.6 km submarine section of the tunnel (Túnel de la Atlántida) ending at 64 m below sea level (Isler 1987). Regarding the islets of the Chinijo archipelago, based on palaeontological criteria, de la Nuez *et al.* (1997) gave ages from the Late Pleistocene to the Holocene.

Discussion

Comparison with previous ages

In Fuerteventura, the normal-polarity magnetozone, which forms the westernmost part of the Southern (Jandía) Shield, gave a younger age of 13.72 ± 0.21 Ma from a lava flow located above a discordance near the highest point of the Cofete track (220 m asl) (cross-sections 4–4’ in Fig. 4 and A–A’ in Fig. 13). The most likely explanation of this youngest volcanic sequence is its relationship to the seamounts located just west of the Jandía peninsula, particularly the Banquete Seamount, a shallow western prolongation of Fuerteventura (see Fig. 1b). These seamounts were dated at 15.3 ± 0.4 and 13.1 ± 0.3 Ma by Ancochea and Huertas (2003) and, according to these researchers, are similar in composition and coeval with the nearby Jandía peninsula. Volcanic activity on the submarine edifices is thought to have ceased at about 13 Ma, coinciding with the construction of the younger normal-polarity sequence of the Southern (Jandía) Shield.

According to previous studies, there are similitudes between the Northern (La Oliva) Shield of Fuerteventura and the Southern (Los Ajaches) Shield of Lanzarote. The main construction stage of Los Ajaches in Lanzarote (Balcells Herrera *et al.* 2006*b*) coincided with the late shield period of the northern part of Fuerteventura (Balcells Herrera *et al.* 2006*a*).

In Lanzarote, the Northern (Famara) Shield ages show significant discrepancies with previously reported data, particularly at the lower section of Famara at Punta Fariones (Fig. 15). The age of 10.89 ± 0.23 Ma SW of Famara cliff is in good agreement with another of 10.2 ± 0.4 Ma from a lava flow of the same basal sequence (Coello *et al.* 1992). However, the ages reported from lavas below and above the calcarenite bed at Punta Fariones are at odds with this sedimentary layer. Coello *et al.* (1992) reported two ages of 6.0 ± 0.4 and 5.3 ± 0.3 Ma from lavas below these sediments, and dated a flow located 50 m above at 9.0 ± 0.3 Ma. In contrast, Abdel-Monem *et al.* (1971) obtained an average age for this horizon of 10.60 ± 1.12 Ma (see Fig. 15). Discrepancies in the stratigraphic correlation of ages in these volcanic sequences of the Northern (Famara) Shield were analysed by Abdel-Monem *et al.* (1971); in particular, replicate samples of their sample LZ-4 from two different sampling points gave results, according to these researchers, whose reproducibility was rather poor owing to the alteration observed for these samples and consequent possible significant argon loss.

Mansour *et al.* (2023) presented a set of radiometric ages of sedimentary, plutonic and volcanic rocks of the Basal Complex of Fuerteventura, which allowed them to delimit the proposed giant landslide of Stillman (1999) affecting the Northern and Central Basal Complex at about 20 Ma, and identified another possible second giant landslide at about 16 Ma affecting the East–Central Basal Complex. It should be noted that the proposed age for the first giant landslide coincides with the beginning of the subaerial growth of the Central (Tuineje) Shield of Fuerteventura, according to the radiometric ages presented in this paper. Likewise, the age for the second giant landslide, further south from the previous one, is

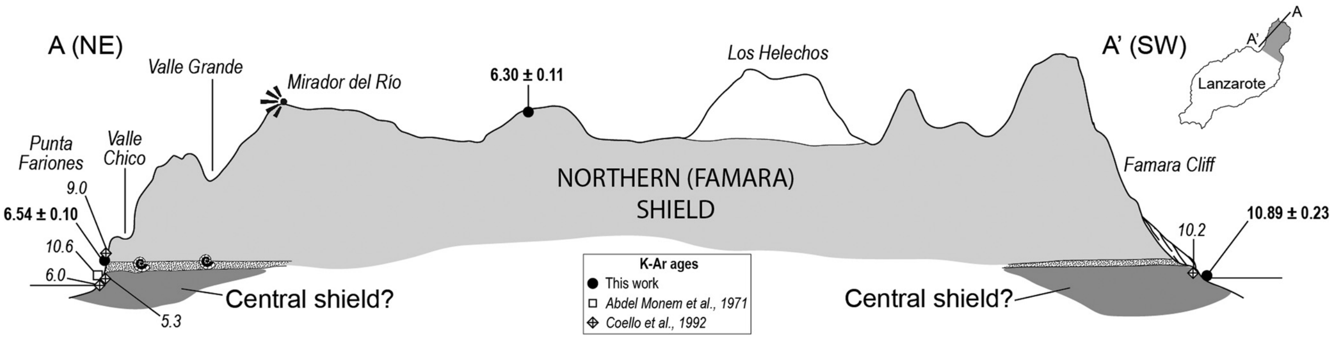

Fig. 15. Idealized cross-section, nonlinear and vertical scale exaggerated, along Famara cliff, northern Lanzarote. Ages obtained along this cliff show significant discrepancies with previously reported data (Abdel-Monem *et al.* 1971; Coello *et al.* 1992), particularly the ages from lavas below and above the fossil-bearing calcarenite bed at Punta Fariones. Ages in Ma.

slightly earlier than the beginning of the volcanic activity in the Southern (Jandía) Shield of Fuerteventura.

Duration and pattern distribution of shield stage

The development of the shields in Fuerteventura and Lanzarote repeats, in terms of duration and distribution, similar patterns to those observed in the shield volcanoes of the other Canaries, with a similar concentration of eruptions in the initial phases (Carracedo 1999; Carracedo *et al.* 2001, 2002; Guillou *et al.* 2004*a*; Paris *et al.* 2005). Radiometric dating of the field-defined magnetozones showed, in general, ages coherent with their relative stratigraphic positions and geomagnetic polarities, constraining the three shields forming both Fuerteventura and Lanzarote.

The long shield growth of the Eastern Canaries is noteworthy, at *c.* 7.1 myr for Fuerteventura and *c.* 9.3 myr for Lanzarote (see Tables 1 and 2, Figs 10, 11 and 14), as is their persistence above sea level for more than 20 myr. They had a relatively long active period compared with intraplate oceanic island lifespans. The development of oceanic island shields is generally restricted to a few million years. For example, submerged islands in the Galapagos or Hawaii are as young as *c.* 6–7 Ma (e.g. Clague and Sherrod 2014; Schwartz *et al.* 2020). For Polynesian and Hawaiian volcanism, the duration of the shield stage is about 1 myr (Guillou *et al.* 1997, 2000, 2014; Garcia *et al.* 2010; Révillon *et al.* 2017; Williamson *et al.* 2019). This large difference in duration is explained by a strong contrast in the drift velocities of the two tectonic plates (i.e. 10 cm a^{-1} for the Pacific plate compared with 2 cm a^{-1} for the African plate).

A comparison of all four Macaronesian archipelagos shows that they share a hotspot origin, despite the Azores being located close to the Mid-Atlantic Ridge whereas the other three island clusters are along the NW African coast resting on the old oceanic crust (e.g. Montelli *et al.* 2006; Jeffery and Gertisser 2018; Carracedo and Troll 2021).

Alternative explanations relate the Canary volcanism and the island's age progression to propagating tensional fractures (Anguita and Hernan 1975; Anguita and Hernán 2000). These alternative versions may explain second-order features such as the alignment of eruptive centres and extended fractures. However, they cannot adequately account for more critical issues, particularly the capacity to generate magma with sufficient volume and persistence to build the Canaries and their composition, associated with ocean island basalt (OIB) magmas.

The hotspot model explains well the origin of the Macaronesian archipelagos, including the Canary Islands. Now, with the accurate and precise chronological framework we have developed for the entire archipelago, combining magnetostratigraphy and unspiked K–Ar dating, we can also assess the extent to which the hotspot hypothesis is appropriate to explain the similar but smaller-scale temporal and spatial distribution pattern; namely, in the progressive coalescence of the shield volcanoes of Fuerteventura and Lanzarote. The initial stages of the successive shields of these two islands occur at different times (Figs 10, 11 and 14) and form discrete, successive and frequently overlapping volcanic edifices (Figs 2, 3 and 16).

The Canary shield stage is much longer than in other volcanic ocean islands because this archipelago formed on a slowly drifting plate (i.e. 2 cm a^{-1}; Carracedo and Troll 2016, 2021) over a hotspot. For comparison, this speed is more than five times slower than the drift speed of the Pacific plate (*c.* 10.5 cm a^{-1}, Chauvel *et al.* 2012).

Another interesting question is why these oceanic chains are formed by separated edifices and not just a continuous volcanic trail

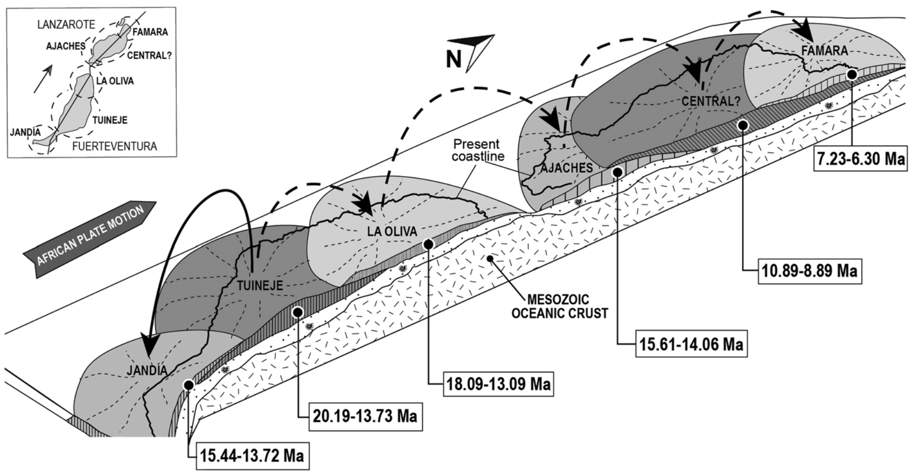

Fig. 16. K–Ar ages indicate that the main bulk of Fuerteventura and Lanzarote is formed by adjacent basaltic shield volcanoes, with a general SW–NE trend. Only Fuerteventura's Southern (Jandía) shield developed SW of the initial Central (Tuineje) shield, built according to the hotspot model in the African plate motion setting.

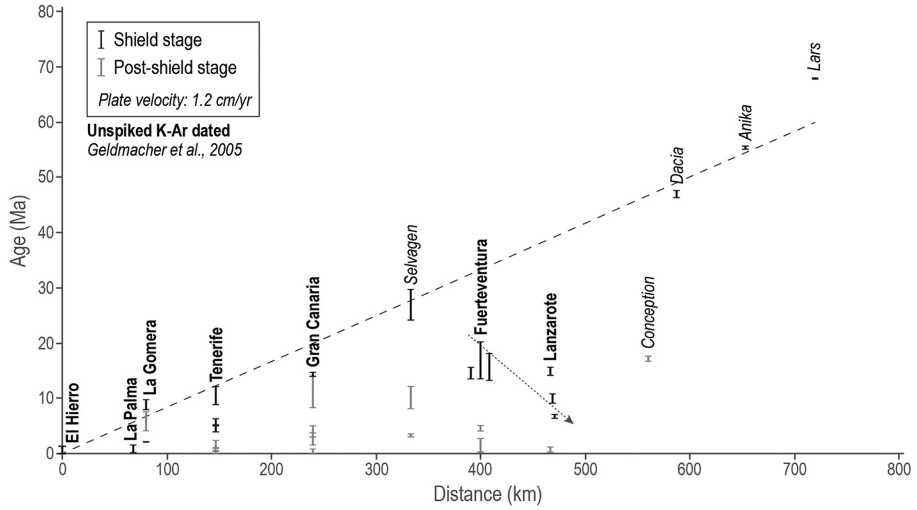

Fig. 17. Ages and distribution of the islands and seamounts of the Canary Volcanic Province, with indication of the plate motion line of 1.2 cm a^{-1}. It should be noted how the Fuerteventura and Lanzarote's shields alignment follow a pattern opposite to this plate motion with the only exception being the Southern (Jandía) Shield of Fuerteventura.

in this very slow plate motion context. The large-scale geometry and age progression of many hotspot island chains, such as the Hawaiian archipelago, are well explained by the steady movement of tectonic plates over stationary hotspots that construct discrete volcanic islands. Plate displacement eventually decouples the island from the magma source, and a new island begins to form at a distance believed to correlate with the lithospheric thickness (Vogt 1974; ten Brink 1991).

Another issue is to understand why the islands are frequently formed by more than one shield volcano, often three in the Canary Islands, and not always following an age progression pattern (Fig. 17). For example, in Tenerife, the first shield to form was the 11.85 ± 0.24 to 8.85 ± 0.18 Ma Central (Roque del Conde) Shield, followed about 2.8 myr later by the 6.07 ± 0.12 to 5.08 ± 0.10 Ma Western (Teno) Shield volcano. The Western (Teno) Shield developed at the western side of the former and, therefore, in a location roughly compatible with the expected displacement of the African plate. Nevertheless, the succeeding 4.87 ± 0.10 to 3.94 ± 0.08 Ma Eastern (Anaga) Shield, located eastwards of the Central (Roque del Conde) Shield, conflicts with the plate progression and a simple hotspot model (Guillou *et al.* 2004*a*). In the Eastern Canaries, the successive shields grew following a similar pattern, becoming consistently younger (except for Jandía) in an NNE direction, at odds with the plate motion and the corresponding pattern of age progression (Figs 16 and 17).

A different approach to explain the shields' arrangement on Fuerteventura and Lanzarote could be related to their growth and gravitational effects. A volcano cannot grow indefinitely. Eventually, as its height increases, there will be a limit preventing further lava erupting from the summit. Shields in the Canaries, built from dense basaltic magmas, rarely reach 1500–2000 m from base to summit. Basaltic magmas are dense fluids, and the pressure required for magma to ascend to the surface must surpass the increasing lithostatic pressure as a shield volcano grows, establishing a density filter as the height of the volcano increases (Pinel and Jaupart 2000; Longpré *et al.* 2009; Castruccio *et al.* 2017). Too much height may force the magma to migrate laterally to build a new volcano (Pinel and Jaupart 2000; Varugu and Amelung 2021; Pinel *et al.* 2022). Instead, the magmatic differentiation working parallel with edifice growth tends to produce less dense magma. Thus, magmas with a sufficiently low density and adequate pressure conditions can reach the surface, favouring eruption (Pinel and Jaupart 2004; Boulesteix *et al.* 2012). For example, phonolitic magmas can produce eruptions from summit craters exceeding 3700 m asl at the Teide Volcano in Tenerife. We postulate that if the supply of dense, basaltic lava continues and the critical limit is reached, lateral pressure will force the growth of another volcano in the periphery. The repetition of this process can give place to a dispersion of shields but rarely to a uniformly aligned distribution, as shown by the Fuerteventura–Lanzarote chain of shield volcanoes (Fig. 16).

This orderly geometry will be feasible if activity migrates in the same direction as the volcanic front advances. Examples of this dispersal are common in developing directional alignments of cinder cones. Some examples consistently progressing southwards in the Canaries are the 1730–36 historical eruption on Lanzarote (Carracedo *et al.* 1992), the progression of the Taburiente Shield on La Palma, forming the Bejenado composite volcano, and the rift-type Cumbre Vieja Ridge, also on La Palma (Carracedo *et al.* 1999, 2001). A combination of a critical growth limit and a propagating volcanic front might be an adequate model to explain the arrangement of shield volcanoes in the Fuerteventura–Lanzarote oceanic ridge, which is opposite in general to the hotspot island's stepwise formation.

Local tectonic activity as well as giant landslides can also play an important role. Gutiérrez *et al.* (2006) indicated an extensional episode with large-scale faulting of WNW and subordinate NNE direction affecting the island of Fuerteventura during its submarine growth. This tectonic geometry could help to guide the postulated propagating volcanic front to the NNE. On the other hand, the possible giant landslide identified by Mansour *et al.* (2023) at around 16 Ma could be the origin of a sudden decompression in the Central (Tuineje) Shield of Fuerteventura that forced a reordering of its magmatic system, which led to the growth of the Southern (Jandía) Shield in the opposite direction to the shield's propagation (Fig. 16).

Conclusions

Determination of geomagnetic polarities, a feature that can be assessed directly on-site using portable flux-gate magnetometers, is a practical tool to define magnetostratigraphic units, which can be used to select the appropriate samples for radiometric dating. Radiometric ages obtained from lavas from Fuerteventura and Lanzarote basaltic shields are generally concordant with their geomagnetic polarity and stratigraphic positions.

Our magnetic and geochronological set of data provides evidence that Fuerteventura and Lanzarote have developed similar patterns to the Central and Western Canaries, constructing adjacent, successively overlapping basaltic shield volcanoes. Cross-sections through these islands confirm that the bulk of the island edifices is formed mainly by Miocene basaltic shields, from 20.19 ± 0.30 to 6.30 ±

0.11 Ma. These ages are consistent with previously published ages but more precise, and we consider them more accurate, with a few exceptions analysed in the text.

The ages and polarities of volcanic units on Lanzarote suggest the occurrence of a central shield. The Basal Unit of the Northern (Famara) Shield probably corresponds to prolonging the Central Shield, whereas a basalt flow unconformably overlying lavas of the Southern (Los Ajaches) Shield points to a flow extending from the Central Shield.

The rejuvenated, post-Miocene volcanic rocks, although forming only a small fraction in volume, cover an extensive part of the islands, hindering the definition of the extent and interrelationship of the shields.

The successive construction of shields is concordant with the general SW–NE trend of the islands, opposite to the Canarian hotspot-induced island progression. We postulate that the shield disposition can be related to gravitational collapses, which forced volcanism to migrate to the periphery of the basaltic shield when exceeding a given density filter, combined with a propagating volcanic front or fracture to account for their contrasting growth directions.

Scientific editing by Nick Varley

Acknowledgements This study was conducted in the Research Consolidated Groups GEOVOL (Canary Islands Government, ULPGC).

Author contributions **FJP-T**: conceptualization (equal), investigation (equal), methodology (equal), writing – original draft (equal); **JCC**: conceptualization (equal), investigation (equal), methodology (equal), writing – original draft (equal); **HG**: data curation (lead), investigation (equal), methodology (equal), writing – original draft (equal); **AR-G**: investigation (equal), writing – original draft (equal); **JLF-T**: investigation (supporting), writing – original draft (supporting), writing – review & editing (supporting)

Funding The geochronological study was supported by the French Atomic Commission (CEA), Centre National de la Recherche Scientifique (CNRS).

Data availability The datasets generated during the current study are available from the corresponding author on request.

Competing interests The authors declare that they have no known competing financial interests or personal relationships that could have appeared to influence the work reported in this paper.

References

Abdel-Monem, A., Watkins, N.D. and Gast, P.W. 1971. Potassium–argon ages, volcanic stratigraphy, and geomagnetic polarity history of the Canary Islands; Lanzarote, Fuerteventura, Gran Canaria, and La Gomera. *American Journal of Science*, **271**, 490–521, https://doi.org/10.2475/ajs.271.5.490

Abdel-Monem, A., Watkins, N.D. and Gast, P.W. 1972. Potassium–argon ages, volcanic stratigraphy, and geomagnetic polarity history of the Canary Islands; Tenerife, La Palma and Hierro. *American Journal of Science*, **272**, 805–825, https://doi.org/10.2475/ajs.272.9.805

Ancochea, E. and Huertas, M.J. 2003. Age and composition of the Amanay Seamount, Canary Islands. *Marine Geophysical Researches*, **24**, 161–169, https://doi.org/10.1007/s11001-004-1100-7

Ancochea, E., Fuster, J. *et al.* 1990. Volcanic evolution of the island of Tenerife (Canary Islands) in the light of new K–Ar data. *Journal of Volcanology and Geothermal Research*, **44**, 231–249, https://doi.org/10.1016/0377-0273(90)90019-C

Ancochea, E., Brändle, J.L., Cubas, C.R., Hernán, F. and Huertas, M.J. 1993. La Serie I de la isla de Fuerteventura. *Memorias de la Real Academia de Ciencias Exactes, Fisicas y Naturales, Madrid*, **27**, 1–151.

Ancochea, E., Hernán, F., Cendrero, A., Cantagrel, J.M., Fúster, J., Ibarrola, E. and Coello, J. 1994. Constructive and destructive episodes in the building of a young Oceanic Island, La Palma, Canary Islands, and genesis of the Caldera de Taburiente. *Journal of Volcanology and Geothermal Research*, **60**, 243–262, https://doi.org/10.1016/0377-0273(94)90054-X

Ancochea, E., Brändle, J.L., Cubas, C.R., Hernán, F. and Huertas, M.J. 1996. Volcanic complexes in the eastern ridge of the Canary Islands: the Miocene activity of the island of Fuerteventura. *Journal of Volcanology and Geothermal Research*, **70**, 183–204, https://doi.org/10.1016/0377-0273(95)00051-8

Ancochea, E., Hernán, F., Huertas, M.J., Brändle, J.L. and Herrera, R. 2006. A new chronostratigraphical and evolutionary model for La Gomera: implications for the overall evolution of the Canarian Archipelago. *Journal of Volcanology and Geothermal Research*, **157**, 271–293, https://doi.org/10.1016/j.jvolgeores.2006.04.001

Anguita, F. and Hernan, F. 1975. A propagating fracture model versus a hot spot origin for the Canary islands. *Earth and Planetary Science Letters*, **27**, 11–19, https://doi.org/10.1016/0012-821X(75)90155-7

Anguita, F. and Hernán, F. 2000. The Canary Islands origin: a unifying model. *Journal of Volcanology and Geothermal Research*, **103**, 1–26, https://doi.org/10.1016/S0377-0273(00)00195-5

Balcells Herrera, R., Barrera Morate, J.L., Gómez Sainz de Aja, J.A., Cueto, L.A., Ancochea, E., Huertas, M.J. and Snelling, N. 1994. Volcanoestratigrafía y edad de la Serie I de Fuerteventura, Islas Canarias. *Boletín Geológico y Minero*, **105**, 50–56.

Balcells Herrera, R., Barrera Morate, J.L. and Gómez Sainz de Aja, J.A. 2006*a*. *Fuerteventura, 92: Mapa Geológico de España Escala 1:100.000*. Instituto Geológico y Minero de España.

Balcells Herrera, R., Barrera Morate, J.L., Gómez Sainz de Aja, J.A. and Ruiz García, M.T. 2006*b*. *Lanzarote, 88: Mapa Geológico de España Escala 1:100.000*. Instituto Geológico y Minero de España.

Balogh, K., Ahijado, A., Casillas, R. and Fernández, C. 1999. Contributions to the chronology of the Basal Complex of Fuerteventura, Canary Islands. *Journal of Volcanology and Geothermal Research*, **90**, 81–101, https://doi.org/10.1016/S0377-0273(99)00008-6

Boulesteix, T., Hildenbrand, A., Gillot, P.-Y. and Soler, V. 2012. Eruptive response of oceanic islands to giant landslides: new insights from the geomorphologic evolution of the Teide–Pico Viejo volcanic complex (Tenerife, Canary). *Geomorphology*, **138**, 61–73, https://doi.org/10.1016/j.geomorph.2011.08.025

Carracedo, J.C. 1979. *Paleomagnetismo e Historia Volcánica de Tenerife*. Aula de Cultura de Tenerife, 1–82.

Carracedo, J.C. 1999. Growth, structure, instability and collapse of Canarian volcanoes and comparisons with Hawaiian volcanoes. *Journal of Volcanology and Geothermal Research*, **94**, 1–19, https://doi.org/10.1016/S0377-0273(99)00095-5

Carracedo, J.C. and Rodriguez Badiola, E. 1993. Evolución geológica y magmática de la isla de Lanzarote, Islas Canarias. *Revista de la Academia Canaria de Ciencias*, **4**, 25–58.

Carracedo, J.C. and Soler, V. 1995. Anomalously shallow palaeomagnetic inclinations and the question of the age of the Canarian Archipelago. *Geophysical Journal International*, **122**, 393–406, https://doi.org/10.1111/j.1365-246X.1995.tb07003.x

Carracedo, J.C. and Troll, V.R. 2016. *The Geology of the Canary Islands*, 1st edn. Elsevier, 1–636.

Carracedo, J.C. and Troll, V.R. 2021. North-East Atlantic Islands: the Macaronesian archipelagos. *In*: Alderton, D. and Elias, S.A. (eds) *Encyclopedia of Geology*, 2nd edn., Elsevier, 674–699.

Carracedo, J.C., Rodriguez Badiola, E. and Soler, V. 1992. The 1730–1736 eruption of Lanzarote, Canary Islands: a long, high-magnitude basaltic fissure eruption. *Journal of Volcanology and Geothermal Research*, **53**, 239–250, https://doi.org/10.1016/0377-0273(92)90084-Q

Carracedo, J.C., Day, S.J., Guillou, H. and Gravestock, P. 1999. Later stages of volcanic evolution of La Palma, Canary Islands: rift evolution, giant landslides, and the genesis of the Caldera de Taburiente. *Geological Society of America Bulletin*, **111**, 755–768, https://doi.org/10.1130/0016-7606(1999)111%3C0755:LSOVEO%3E2.3.CO;2

Carracedo, J.C., Badiola, E.R., Guillou, H., de la Nuez, J. and Perez-Torrado, F.J. 2001. Geology and volcanology of La Palma and El Hierro, Western Canaries. *Estudios Geológicos*, **57**, 175–273, https://doi.org/10.3989/egeol.01575-6134

Carracedo, J.C., Perez-Torrado, F.J. *et al.*. 2002. Cenozoic volcanism II: the Canary Islands. *In*: Gibbons, W. and Moreno, T. (eds) *The Geology of Spain*. Geological Society, London, 439–472.

Carracedo, J.C., Singer, B. *et al.* 2003. La erupción y el tubo volcánico del Volcán Corona (Lanzarote, Islas Canarias). *Estudios Geológicos*, **59**, 277–302, https://doi.org/10.3989/egeol.03595-6104

Carracedo, J.C., Rodríguez Badiola, E. *et al.* 2007. Eruptive and structural history of Teide Volcano and rift zones of Tenerife, Canary Islands. *Geological Society of America Bulletin*, **119**, 1027–1051, https://doi.org/10.1130/B26087.1

Casillas, R. and Martin, G. 2021. Estructura y evolución del Edificio Volcánico Mioceno de Jandía (Fuerteventura, Islas Canarias). *Geogaceta*, **69**, 31–34.

Castruccio, A., Diez, M. and Gho, R. 2017. The influence of plumbing system structure on volcano dimensions and topography. *Journal of Geophysical Research: Solid Earth*, **122**, 8839–8859, https://doi.org/10.1002/2017JB014855

Chauvel, C., Maury, R.C. *et al.* 2012. The size of plume heterogeneities constrained by Marquesas isotopic stripes. *Geochemistry, Geophysics, Geosystems*, **13**, Q07005, https://doi.org/10.1029/2012GC004123

Clague, D.A. and Dalrymple, G.B. 1987. The Hawaiian–Emporer volcanic chain. Part I – geologic evolution. *US Geological Survey, Professional Papers*, **1350**, 5–54.

Clague, D.A. and Sherrod, D.R. 2014. Growth and degradation of Hawaiian volcanoes. *US Geological Survey, Professional Papers*, **1801**, 97–146.

Coello, J., Cantagrel, J.M. *et al.* 1992. Evolution of the eastern volcanic ridge of the Canary Islands based on new K–Ar data. *Journal of Volcanology and Geothermal Research*, **53**, 251–274, https://doi.org/10.1016/0377-0273(92)90085-R

de la Nuez, J., Quesada, M.L. and Alonso, J.J. 1997. *Los volcanes de los islotes al norte de Lanzarote: Islas Canarias*. Fundacion Cesar Manrique, Lanzarote, 1–223.

EMODnet Bathymetry Consortium 2020. EMODnet Digital Bathymetry (DTM 2020), https://doi.org/10.12770/bb6a87dd-e579-4036-abe1-e649cea9881a

Féraud, G., Giannérini, G., Campredon, R. and Stillman, C.J. 1985. Geochronology of some Canarian dike swarms: contribution to the volcano-tectonic evolution of the archipelago. *Journal of Volcanology and Geothermal Research*, **25**, 29–52, https://doi.org/10.1016/0377-0273(85)90003-4

Fernandez, C., Casillas, R., Ahijado, A., Perello, V. and Hernandez-Pacheco, A. 1997. Shear zones as a result of intraplate tectonics in oceanic crust: the example of the Basal complex of Fuerteventura (Canary Islands). *Journal of Structural Geology*, **19**, 41–57, https://doi.org/10.1016/S0191-8141(96)00074-0

Fúster, J.M. and Carracedo, J.C. 1979. Magnetic polarity mapping of Quaternary volcanic activity of Fuerteventura and Lanzarote (Canary Islands). *Estudios Geológicos*, **35**, 59–65.

Fúster, J.M., Cendrero, A., Gastesi, P., Ibarrola, E. and Ruiz, J.L. 1968*a*. *Geología y volcanología de las Islas Canarias: Fuerteventura*. Instituto Lucas Mallada (CSIC), Madrid, 1–239.

Fúster, J.M., Santin, S.F. and Sagredo, A. 1968*b*. *Geología y volcanología de las Islas Canarias: Lanzarote*. Instituto Lucas Mallada (CSIC), Madrid, 1–177.

Garcia, M.O., Swinnard, L., Weis, D., Greene, A.R., Tagami, T., Sano, H. and Gandy, C.E. 2010. Petrology, geochemistry and geochronology of Kaua'i Lavas over 4·5 Myr: implications for the origin of rejuvenated volcanism and the evolution of the Hawaiian plume. *Journal of Petrology*, **51**, 1507–1540, https://doi.org/10.1093/petrology/egq027

Geldmacher, J., Hoernle, K., Bogaard, P.v.d., Duggen, S. and Werner, R. 2005. New ^{40}Ar/^{39}Ar age and geochemical data from seamounts in the Canary and Madeira volcanic provinces: support for the mantle plume hypothesis. *Earth and Planetary Science Letters*, **237**, 85–101, https://doi.org/10.1016/j.epsl.2005.04.037

Gradstein, F.M., Ogg, J.G., Schmitz, M.D. and Ogg, G.M. (eds) 2020. *Geologic Time Scale 2020*, Elsevier, https://doi.org/10.1016/B978-0-12-824360-2.00032-2

Guillou, H., Carracedo, J.C., Perez-Torrado, F.J. and Rodríguez Badiola, E. 1996. K–Ar ages and magnetic stratigraphy of a hotspot-induced, fast grown oceanic island: El Hierro, Canary Islands. *Journal of Volcanology and Geothermal Research*, **73**, 141–155, https://doi.org/10.1016/0377-0273(96)00021-2

Guillou, H., Garcia, M.O. and Turpin, L. 1997. Unspiked K–Ar dating of young volcanic rocks from Loihi and Pitcairn hot spot seamounts. *Journal of Volcanology and Geothermal Research*, **78**, 239–249, https://doi.org/10.1016/S0377-0273(97)00012-7

Guillou, H., Carracedo, J.C. and Day, S.J. 1998. Dating of the Upper Pleistocene–Holocene volcanic activity of La Palma using the unspiked K–Ar technique. *Journal of Volcanology and Geothermal Research*, **86**, 137–149, https://doi.org/10.1016/S0377-0273(98)00074-2

Guillou, H., Sinton, J., Laj, C., Kissel, C. and Szeremeta, N. 2000. New K–Ar ages of shield lavas from Waianae Volcano, Oahu, Hawaiian Archipelago. *Journal of Volcanology and Geothermal Research*, **96**, 229–242, https://doi.org/10.1016/S0377-0273(99)00153-5

Guillou, H., Carracedo, J.C. and Duncan, R.A. 2001. K–Ar, ^{40}Ar–^{39}Ar ages and magnetostratigraphy of Brunhes and Matuyama lava sequences from La Palma Island. *Journal of Volcanology and Geothermal Research*, **106**, 175–194, https://doi.org/10.1016/S0377-0273(00)00294-8

Guillou, H., Carracedo, J.C., Paris, R. and Perez-Torrado, F.J. 2004*a*. Implications for the early shield-stage evolution of Tenerife from K/Ar ages and magnetic stratigraphy. *Earth and Planetary Science Letters*, **222**, 599–614, https://doi.org/10.1016/j.epsl.2004.03.012

Guillou, H., Perez-Torrado, F.J., Hansen, A., Carracedo, J.C. and Gimeno, D. 2004*b*. The Plio-Quaternary volcanic evolution of Gran Canaria based on new K–Ar ages and magnetostratigraphy. *Journal of Volcanology and Geothermal Research*, **135**, 221–246, https://doi.org/10.1016/j.jvolgeores.2004.03.003

Guillou, H., Nomade, S., Carracedo, J.C., Kissel, C., Laj, C., Perez Torrado, F.J. and Wandres, C. 2011. Effectiveness of combined unspiked K–Ar and ^{40}Ar/^{39}Ar dating methods in the ^{14}C age range. *Quaternary Geochronology*, **6**, 530–538, https://doi.org/10.1016/j.quageo.2011.03.011

Guillou, H., Maury, R.C. *et al.* 2014. Volcanic successions in Marquesas eruptive centers: a departure from the Hawaiian model. *Journal of Volcanology and Geothermal Research*, **276**, 173–188, https://doi.org/10.1016/j.jvolgeores.2013.12.003

Gutiérrez, M., Casillas, R. *et al.* 2006. The submarine volcanic succession of the basal complex of Fuerteventura, Canary Islands: a model of submarine growth and emergence of tectonic volcanic islands. *Geological Society of America Bulletin*, **118**, 785–804, https://doi.org/10.1130/B25821.1

Hausen, H.M. 1959. On the geology of Lanzarote, Graciosa and the Isletas (Canarian Archipelago). *Societas Scientiarum Fennica Commentationes Physico Mathematicae*, **23**, 1–116.

Hausen, H.M. 1967. Sobre el desarrollo geológico de Fuerteventura, Islas Canarias. Una breve reseña. *Anuario de Estudios Atlanticos*, **13**, 11–37.

Isler, O. 1987. Expedition internationale 1986 au tunnel de l'Atlantida: Canaries. *Spelunca Bulletin*, **25**, 25–30.

Jeffery, A.J. and Gertisser, R. 2018. Peralkaline felsic magmatism of the Atlantic Islands. *Frontiers in Earth Science*, **6**, 1–42, https://doi.org/10.3389/feart.2018.00145

Kissel, C., Guillou, H., Laj, C., Carracedo, J.C., Nomade, S., Perez-Torrado, F. and Wandres, C. 2011. The Mono Lake excursion recorded in phonolitic lavas from Tenerife (Canary Islands): paleomagnetic analyses and coupled K/Ar and Ar/Ar dating. *Physics of the Earth and Planetary Interiors*, **187**, 232–244, https://doi.org/10.1016/j.pepi.2011.04.014

Kissel, C., Guillou, H. *et al.* 2014. A combined paleomagnetic/dating investigation of the upper Jaramillo transition from a volcanic section at Tenerife (Canary Islands). *Earth and Planetary Science Letters*, **406**, 59–71, https://doi.org/10.1016/j.epsl.2014.09.003

Kissel, C., Rodriguez-Gonzalez, A., Laj, C., Perez-Torrado, F., Carracedo, J.C., Wandres, C. and Guillou, H. 2015. Paleosecular variation of the earth magnetic field at the Canary Islands over the last 15 ka. *Earth and Planetary Science Letters*, **412**, 52–60, https://doi.org/10.1016/j.epsl.2014.12.031

Klug, H. 1968. *Morphologische Studien auf den Kanarischen Lnseln*. Beiträge zur Küstenentwicklung und Talbildung auf einen Vulkanischen Archipiel, **3**.

Krastel, S., Schmincke, H.-U., Jacobs, C.L., Rihm, R., Le Bas, T.P. and Alibés, B. 2001. Submarine landslides around the Canary Islands. *Journal of Geophysical Research: Solid Earth*, **106**, 3977–3997, https://doi.org/10.1029/2000JB900413

Lecointre, G., Tinkler, K.J. and Richards, H.G. 1967. The marine Quaternary of the Canary Islands. *Proceedings of the Academy of Natural Sciences of Philadelphia*, **119**, 325–344.

Longpré, M.-A., Troll, V.R., Walter, T.R. and Hansteen, T.H. 2009. Volcanic and geochemical evolution of the Teno massif, Tenerife, Canary Islands: some repercussions of giant landslides on ocean island magmatism. *Geochemistry, Geophysics, Geosystems*, **10**, https://doi.org/10.1029/2009GC002892

Longpré, M.-A., Chadwick, J.P., Wijbrans, J. and Iping, R. 2011. Age of the El Golfo debris avalanche, El Hierro (Canary Islands): new constraints from laser and furnace ^{40}Ar/^{39}Ar dating. *Journal of Volcanology and Geothermal Research*, **203**, 76–80, https://doi.org/10.1016/j.jvolgeores.2011.04.002

Mansour, S., Glasmacher, U.A., Krob, F.C., Casillas, R. and Albinger, M. 2023. Timing of rapid cooling and erosional decay of two volcanic islands of the Canary Archipelago: implications from low-temperature thermochronology. *International Journal of Earth Sciences*, **112**, 345–382, https://doi.org/10.1007/s00531-022-02253-7

Martínez Puebla, E., Prieto Ruiz, J. and Centellas Bodas, A. 2005. *Guía de Visita del Parque Nacional de Timanfaya*. Organismo Autónomo Parques Nacionales, 1–158.

McDougall, I. and Schmincke, H.-U. 1976. Geochronology of Gran Canaria, Canary Islands: age of shield building volcanism and other magmatic phases. *Bulletin Volcanologique*, **40**, 57–77, https://doi.org/10.1007/BF02599829

Meco, J. and Stearns, C.E. 1981. Emergent littoral deposits in the eastern Canary Islands. *Quaternary Research*, **15**, 199–208, https://doi.org/10.1016/0033-5894(81)90104-6

Meco, J., Scaillet, S. *et al.* 2007. Evidence for long-term uplift on the Canary Islands from emergent Mio–Pliocene littoral deposits. *Global and Planetary Change*, **57**, 222–234, https://doi.org/10.1016/j.gloplacha.2006.11.040

Montelli, R., Nolet, G., Dahlen, F.A. and Masters, G. 2006. A catalogue of deep mantle plumes: new results from finite-frequency tomography. *Geochemistry, Geophysics, Geosystems*, **7**, https://doi.org/10.1029/2006GC001248

Ogg, J.G. 2020. Geomagnetic polarity time scale. *In*: Gradstein, F.M., Ogg, J.G., Schmitz, M.D. and Ogg, G.M. (eds) *Geologic Time Scale 2020*, Elsevier, 159–192, https://doi.org/10.1016/B978-0-12-824360-2.00005-X

Paris, R., Guillou, H., Carracedo, J.C. and Perez-Torrado, F.J. 2005. Volcanic and morphological evolution of La Gomera (Canary Islands), based on new K–Ar ages and magnetic stratigraphy: implications for oceanic island evolution. *Journal of the Geological Society, London*, **162**, 501–512, https://doi.org/10.1144/0016-764904-055

Perez-Torrado, F.J., Carracedo, J.C. and Mangas, J. 1995. Geochronology and stratigraphy of the Roque Nublo Cycle, Gran Canaria, Canary Islands. *Journal of the Geological Society, London*, **152**, 807–818, https://doi.org/10.1144/gsjgs.152.5.0807

Petit-Maire, N., Delibrias, G., Meco, J., Pomel, S. and Rosso, J.C. 1986. Paléoclimatologie des Canaries Orientales (Fuerteventura). *Comptes rendus de l'Académie des Sciences*, **303**, 1241–1246.

Pinel, V. and Jaupart, C. 2000. The effect of edifice load on magma ascent beneath a volcano. *Philosophical Transactions of the Royal Society of London, Series A*, **358**, 1515–1532, https://doi.org/10.1098/rsta.2000.0601

Pinel, V. and Jaupart, C. 2004. Magma storage and horizontal dyke injection beneath a volcanic edifice. *Earth and Planetary Science Letters*, **221**, 245–262, https://doi.org/10.1016/S0012-821X(04)00076-7

Pinel, V., Furst, S., Maccaferri, F. and Smittarello, D. 2022. Buoyancy versus local stress field control on the velocity of magma propagation: insight from analog and numerical modelling. *Frontiers in Earth Science*, **10**, https://doi.org/10.3389/feart.2022.838318

Révillon, S., Guillou, H. *et al.* 2017. Young Marquesas volcanism finally located. *Lithos*, **294–295**, 356–361, https://doi.org/10.1016/j.lithos.2017.10.013

Rodriguez-Gonzalez, A., Perez-Torrado, F.J., Fernandez-Turiel, J.L., Aulinas, M., Paris, R. and Moreno-Medina, C. 2018. The Holocene volcanism of Gran

Canaria (Canary Islands, Spain). *Journal of Maps*, **14**, 620–629, https://doi.org/10.1080/17445647.2018.1526717

Rodriguez-Gonzalez, A., Fernandez-Turiel, J.L. *et al.* 2022. Lava deltas, a key landform in oceanic volcanic islands: El Hierro, Canary Islands. *Geomorphology*, **416**, 108427, https://doi.org/10.1016/j.geomorph.2022.108427

Sánchez-Guzmán, J. and Abad, J. 1986. Sondeo geotérmico Lanzarote-1. *Anales de Física*, **82**, 102–109.

Schwartz, D.M., Wanless, V.D., Soule, S.A., Schmitz, M.D. and Kurz, M.D. 2020. Monogenetic near-island seamounts in the Galápagos archipelago. *Geochemistry, Geophysics, Geosystems*, **21**, e2020GC008914, https://doi.org/10.1029/2020GC008914

SPA-15 1975. *Estudio Científico de Los Recursos de Agua En Las Islas Canarias (SPA/69/515). MOP (DGOH)-PNUD (UNESCO)*. Dirección General de Obras Hidráulicas-UNESCO, Madrid.

Staudigel, H., Feraud, G. and Giannerini, G. 1986. The history of intrusive activity on the island of La Palma (Canary Islands). *Journal of Volcanology and Geothermal Research*, **27**, 299–322, https://doi.org/10.1016/0377-0273(86)90018-1

Stillman, C.J. 1999. Giant Miocene landslides and the evolution of Fuerteventura, Canary Islands. *Journal of Volcanology and Geothermal Research*, **94**, 89–104, https://doi.org/10.1016/S0377-0273(99)00099-2

Stillman, C.J., Bennell-Baker, M.J., Smewing, J.D., Fúster, J.M., Muñoz, M. and Sagredo, J. 1975. Basal complex of Fuerteventura (Canary Islands) is an oceanic intrusive complex with rift-system affinities. *Nature*, **257**, 469–471, https://doi.org/10.1038/257469a0

ten Brink, U. 1991. Volcano spacing and plate rigidity. *Geology*, **19**, 397–400, https://doi.org/10.1130/0091-7613(1991)019%3C0397:VSAPR%3E2.3.CO;2

Thirlwall, M.F., Singer, B.S. and Marriner, G.F. 2000. ^{39}Ar–^{40}Ar ages and geochemistry of the basaltic shield stage of Tenerife, Canary Islands, Spain. *Journal of Volcanology and Geothermal Research*, **103**, 247–297, https://doi.org/10.1016/S0377-0273(00)00227-4

Varugu, B. and Amelung, F. 2021. Southward growth of Mauna Loa's dike-like magma body driven by topographic stress. *Scientific Reports*, **11**, 9816, https://doi.org/10.1038/s41598-021-89203-6

Vogt, P.R. 1974. Volcano spacing, fractures, and thickness of the lithosphere. *Earth and Planetary Science Letters*, **21**, 235–252, https://doi.org/10.1016/0012-821X(74)90159-9

Watkins, N.D. 1973. Palaeomagnetism of the Canary Islands and Madeira. *Geophysical Journal International*, **32**, 249–267, https://doi.org/10.1111/j.1365-246X.1973.tb05830.x

Williamson, N.M.B., Weis, D., Scoates, J.S., Pelletier, H. and Garcia, M.O. 2019. Tracking the geochemical transition between the Kea-dominated Northwest Hawaiian Ridge and the bilateral Loa–Kea trends of the Hawaiian Islands. *Geochemistry, Geophysics, Geosystems*, **20**, 4354–4369, https://doi.org/10.1029/2019GC008451

Zimmerman, E.C. 1948. *Insects of Hawaii. 1. Introduction*. University of Hawaii Press, Honolulu.